Nuclear structure effects and systematics of alpha transitions for $52 \leqslant Z \leqslant 90$

V. M. Vakhtel', N. A. Golovkov, K. Ya. Gromov, R. B. Ivanov, S. G. Kadmenskiĭ, S. D. Kurgalin, M. A. Mikhaĭlova, A. V. Tokmakov, V. I. Furman, and V. G. Chumin

Joint Institute for Nuclear Research, Dubna

Fiz. Elem. Chastits At. Yadra **18**, 777–819 (July–August 1987)

The existing experimental data on α-transition probabilities are analyzed systematically on the basis of the non-R-matrix approach to the theory of α decay. The influence of the nuclear structure on the absolute and relative probabilities of α decay is explained consistently by means of the shell model. Some theoretical predictions stimulating new experiments are made.

INTRODUCTION

The study of α decay is one of the traditional directions of nuclear physics. The results of the experimental and theoretical studies have been systematized in a number of monographs.[1–4] Experimental data on α-transition probabilities together with an analysis of them in accordance with the single-particle theory of α decay are included in the complete list of data on isotopes that are summarized in the periodically published compilations of the type of Ref. 5. In the majority of books[1–3,6] and reviews[7,8] the data are analyzed and systematized by means of the R-matrix theory of α decay, which, albeit with certain limitations, can be claimed to explain [9–14] the relative α-transition probabilities. But it is only on the basis of non-R-matrix variants of α-decay theory that it has proved possible satisfactorily to pose and solve the problem of the absolute α-transition probabilities [4,15–22]

In this review, the formalism and ideas of the non-R-matrix theory of α decay are used to make a detailed analysis of the experimental data so far accumulated. The material presented below augments and develops the results presented in the monograph of Ref. 4.

1. BASIC CHARACTERISTICS OF α DECAY

1. Experimental properties of α transitions

Figure 1 gives the nuclei for which α decay has been discovered experimentally; it includes the comparatively recently obtained neutron-deficient nuclei with $Z = 52$–56.[23,24] For a quarter of these nuclei, only the value of Q_α has been measured; for 10% of the nuclides in the figure, α decay of their isomer states has been observed. In the coming years, we can expect a significant increase in the number of identified α emitters, this being made possible by the development of methods for obtaining strongly neutron-deficient isotopes, in particular in heavy-ion nuclear reactions, and also in deep spallation reactions.

The probability of α decay is determined by the transition energy and the quantum numbers of the initial state i (in the parent nucleus ${}^{A}_{Z}X_N$) and final state f (in the daughter nucleus ${}^{A-4}_{Z-2}Y_{N-2}$). We shall characterize the state i by the spin J_i, parity π_i, and other quantum numbers σ_i. Not only the ground state but also excited states J_f, π_f, σ_f of the daughter nucleus can be populated by α decay. Since the α particle has spin $S_\alpha = 0$, the angular momentum which it carries away is equal to the orbital angular momentum L of the relative motion of the α particle and the daughter nucleus; moreover, the conservation laws for the parity and total spin of the system impose on L the selection rules

$$| J_i - J_f | \leqslant L \leqslant | J_i + J_f | ; \quad \pi_i = (-1)^L \pi_f. \tag{1}$$

The experimentally measured energy E_c of the α particle in channel c, which is determined by the quantum numbers $c \equiv L, J_f, \pi_f, \sigma_f$, can be expressed in terms of the energy Q_c of the relative motion of the α particle and the daughter nucleus, and also the screening energy E_{scr}:

$$E_c = (A - 4)\, Q_c/A - E_{\text{scr}}, \tag{2}$$

where

$$Q_c = Q_0 + E_i^* - E_f^*, \tag{3}$$

and Q_0 corresponds to the transition between the ground states of the parent and daughter nuclei:

$$Q_0 = B_{J_{i0}\pi_{i0}\sigma_{i0}} - B_{J_{f0}\pi_{f0}\sigma_{f0}} - B_\alpha. \tag{4}$$

In Eqs. (3) and (4), E_i^* and E_f^* are the excitation energies of the parent and daughter nuclei, $B_{J_0\pi_0\sigma_0}$ is the binding energy of the ground state of the nuclide, and $B_\alpha = +28.297$ MeV is the binding energy of the α particle. The screening energy (measured in electron volts) in Ref. 3 can be represented in the form[1]

$$E_{\text{scr}} = 64.3\ (Z)^{7/5} - 80\ (Z)^{2/5}. \tag{5}$$

The irregular dependence of Q_c on N and Z can be approximately described[25,26] by the semiempirical nuclear mass formula with inclusion of shell corrections. The presence of the minimum in the values of Q_0 at $Z = 82$ and $N = 124$ and the increase of Q_0 on the transition from the β-stability valley to the neutron-deficient nuclei determine the pronounced asymmetry in the number of studied α-decay nuclei with $\Delta N > 0$ and $\Delta N < 0$ as revealed in Fig. 1.

The α-decay partial widths Γ_c in channel c can be expressed in terms of the total half-life $T_{\frac{1}{2}}$ of the state of the parent nucleus by the relation

$$\Gamma_c = \frac{\hbar \ln 2}{T_{1/2}} \frac{\alpha}{100} \frac{\alpha_c}{100} \equiv \frac{\hbar \ln 2}{T_{1/2c}^{(\alpha)}}, \tag{6}$$

where α is the total fraction of α decay, and $\alpha_c = \Gamma_c/\Gamma_\alpha$ is the fraction of channel c of the total α-decay width $\Gamma_\alpha = \Sigma_c \Gamma_c$ (α and α_c are expressed in percentages).

2. Single-particle model of α decay and the Geiger–Nuttall law

For α transitions between the ground states of even–even nuclei, Geiger and Nuttall found an empirical relationship between the partial half-life $T_{\frac{1}{2}}^{(\alpha)}$ and the energy Q_0:

 0090-4759/87/040331-19$04.40

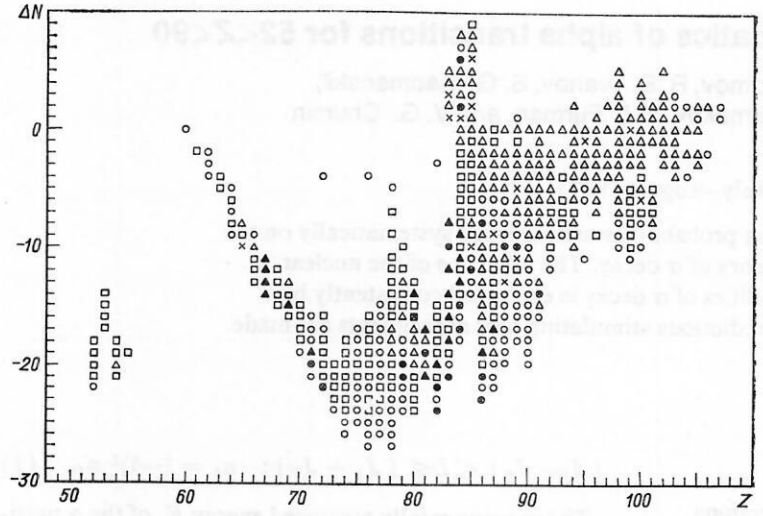

FIG. 1. Alpha-radioactive nuclides. The ordinate ΔN is the difference of the number of neutrons in the given nuclide measured from the value of N of the isotope that lies in the β-stability valley. Notation: open circles, only Q_α and $T_{1/2}$ known; open squares, Q_α, $T_{1/2}$, $T^\alpha_{1/2}$ known; open triangles, Q_α, $T_{1/2}$ $T^\alpha_{1/2}$ known and fine structure (f.s.) of the α spectra detected; open circles with crosses, Q_α and $T_{1/2}$ known and α decay of an isomer state (m) known; black circles, Q_α and $T_{1/2}$ known and f.s.; crosses, Q_α, $T_{1/2}$, and $T^\alpha_{1/2}$ known and f.s. and (m); black triangles, Q_α, $T_{1/2}$, and $T^\alpha_{1/2}$ known and (m).

$$\log T^{(\alpha)}_{1/2} = A(Z) + B(Z)/\sqrt{Q_0}, \tag{7}$$

where $A(Z)$ and $B(Z)$ are Q_0-independent functions. Figure 2a shows the linear dependence of $\log T^{(\alpha)}_{\frac{1}{2}}$ on $Q_0^{-\frac{1}{2}}$ for the Hg, Pt, Po, Rn, Ra, and Th isotopes. It must be emphasized that for the series of Po, Rn, Ra, and Th isotopes, for which the neutron number passes through $N = 126$, two branches of the straight lines (7) are observed, differing both in the slope factors $B(Z)$ and in the values of $A(Z)$, i.e., in fact A and B in (7) depend not only on Z but also on N.

A qualitative explanation of the Geiger–Nuttall law was obtained in Refs. 27 and 28 on the basis of the single-particle variant of α-decay theory, in which the partial width Γ_c has the form

$$\Gamma_c = \hbar \nu_c P_c, \tag{8}$$

where ν_c is the frequency with which the α particle "strikes" the potential barrier, and P_c is the probability of transmission of a pointlike α particle through it. In the semiclassical approximation and for $L = 0$, the probability P_c has the form[2]

$$P_c = \exp\left(-2\pi\eta + 2\eta \arccos\frac{\eta - \rho}{\eta} + 2\rho\tilde{k}\right), \tag{9}$$

where

$$\rho = k_c R_c, \quad \tilde{k} = (2\eta/\rho - 1)^{1/2}, \quad \eta = 2Ze^2/\hbar v_c,$$

and k_c, v_c, and R_c are the wave number, velocity, and radius of channel c, respectively. If (8) and (9) are substituted in (6) and logarithms are taken, an expression with a form close to (7) is obtained, provided ν_c is constant.[2,3]

3. Structure effects in α decay and experimental hindrance factors

If one attempts to construct a dependence like the Geiger–Nuttall law for α transitions from the ground states of odd and odd–odd nuclei, and also for α transitions from excited states of parent nuclei or to excited states of daughter nuclei, then, first, the corresponding points do not lie on the lines corresponding to the α transitions between the ground states of the even–even nuclei and, second, the distribution of these points is irregular. This means that ν_c in Eq. (8) depends nontrivially on the structure of the states of the nuclei connected by the α transition. To characterize this dependence quantitatively, one usually employs the so-called hindrance factors, the standard definition of which is as follows[1-3,5]:

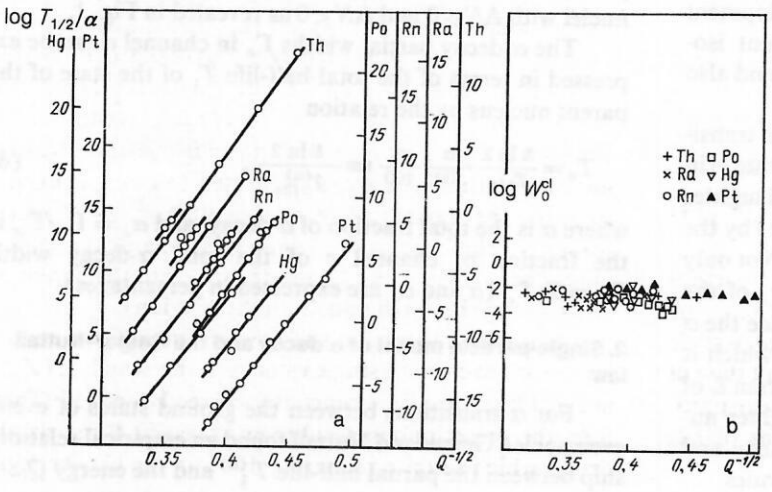

FIG. 2. Dependence on the α-decay energy of the partial half-life $T^\alpha_{1/2}$ (a) and the cluster spectroscopic factors W^{cl}_0 (b) for some even–even isotopes.

$$F_L(\text{e.e.}) = \frac{\Gamma_0(\text{e.e.})}{\Gamma_c(\text{e.e.})}; \tag{10}$$

$$F_L^N(\text{e.o}) = \frac{\Gamma_0(\text{e.o}-1) + \Gamma_0(\text{e.o}+1)}{2\Gamma_c(\text{e.o})}; \tag{11}$$

$$F_L^Z(\text{o.e}) = \frac{\Gamma_0(\text{o}-1.\text{e}) + \Gamma_0(\text{o}+1.\text{e})}{2\Gamma_c(\text{o.e})}; \tag{12}$$

$$F_L^{N\leftarrow}(\text{o.o}) = \frac{\Gamma_0(\text{o}-1.\text{o}-1)\,\Gamma_0(\text{o}+1.\text{o}+1)\Gamma_0(\text{o}-1.\text{o}+1) + \Gamma_0(\text{o}+1.\text{o}-1)}{4\Gamma_c(\text{o.o})}, \tag{13}$$

where the first (respectively, second) index e or o indicates that the number of protons (respectively, neutrons) of the parent nucleus is even or odd.

In Eqs. (10)–(13), Γ_c is the experimental partial width for the investigated α-decay channel c, and Γ_0 is the width calculated in accordance with the expression (7) when one substitutes into it the values of Z and Q_c corresponding to the studied α transition. In the general case, the hindrance factors F_0 are calculated for all α transitions under the assumption that $L = 0$. When the values of L are known, one also calculates the reduced hindrance factors F_L, which take into account the influence of the centrifugal barrier on the width Γ_c.

On the basis of the values of F_0, all α transitions can be divided into three main groups. The first group contains the α transitions with $L = 0$ and $F_0 \leqslant 5$; these are called favored transitions. The second group is formed by the α transitions with $L \neq 0$ and $3 < F_0 \leqslant 100$ (semifavored transitions). The third group includes the α transitions with $L \neq 0$, $10 < F_0 < 1000$ and corresponds to the unfavored α transitions.

Apart from these groups, α transitions with values $F_0 = 10^4$–10^7, corresponding to so-called configuration-forbidden α transitions, are observed experimentally.

A consistent explanation of this classification of α transitions became possible only after the appearance of the many-particle variants of α-decay theory. Indeed, from the point of view of the single-particle theory (8) the hindrance factors F_L (10)–(13) can be expressed in terms of the ratios of the frequencies ν_c for the favored and investigated transitions. The fact that the values of ν_c vary by three orders of magnitude (and more!) cannot, in principle, be understood in the framework of the single-particle approach. To explain the behavior of ν_c, it is necessary to take into account consistently the influence of the state structure of the parent and daughter nuclei on the width Γ_c.

Historically, the first many-particle variant of α-decay theory was the R-matrix variant, in which the theory of nuclear reactions at low energies[29] was used to obtain the following expression for the α-decay width[30]:

$$\Gamma_c = 2k_c \frac{1}{\overline{G}_c^2(R_c)} \gamma_c^2(R_c), \tag{14}$$

where $\overline{G}_c(R_c)$ is an irregular solution of the single-particle Schrödinger equation that takes into account not only the Coulomb but also the nuclear interaction of the α particle with the daughter nucleus, and $\gamma_c(R_c)$ is the amplitude of the reduced α-decay width expressed in terms of the α-particle form factor $\psi_c(R_c)$ [defined below by means of Eq. (16)] by the relation

$$\gamma_c(R_c) = \frac{\hbar}{\sqrt{2MR_c}} \psi_c(R_c), \tag{15}$$

where M is the reduced mass of the α particle, and R_c is the "radius" of channel c.

Using in the expression (14) the experimental values Γ_c^{exp} and calculating the function $\overline{G}_c(R_c)$, one can obtain $\gamma_c^2(R_c)^{\text{exp}}$ and then use them to classify the α transitions. At the present time, two schemes for calculating the $\gamma_c^2(R_c)^{\text{exp}}$ are widely used. If for R_c one chooses the value corresponding to the inner turning point, and $\overline{G}^2(R_c)$ is calculated semiclassically with allowance for the nuclear potential of the α-particle interaction with the daughter nucleus, then $\gamma_c^2(R_c)^{\text{exp}}$ is found to be proportional to the $\delta_c^2(R_c)$ obtained in Ref. 10.

In the other variant[7] for obtaining the reduced widths $\gamma_c^2(R_c)$, the radius R_c is chosen in the form $R_c = 1.55A^{1/3}$ F, and the function $\overline{G}_c(R_c)$ is replaced by the irregular Coulomb function $G_c(R)$, which is calculated in accordance with the semiclassical formulas.

The largest values of $\gamma_c^2(R_c)^{\text{exp}}$ are obtained for favored α transitions between the ground states of even–even nuclei. The relative hindrance of all the remaining α transitions is characterized in the framework of R-matrix theory by the hindrance factors HF_0^{R} (Ref. 6) determined by Eqs. (10)–(13), in which Γ_c and Γ_0 must be replaced by the corresponding reduced widths $\gamma_c^2(R_c)^{\text{exp}}$. The absolute values and the α-transition-type hierarchy of the hindrance factors HF_0^{R} are found to be in reasonable agreement with the analogous characteristics of the hindrance factors F_0 introduced above.

The behavior of the quantities $\gamma_c^2(R_c)^{\text{exp}}$ as functions of N, Z, and the α-transition type, and, therefore, the behavior of the hindrance factors HF_0^{R}, can be compared with the corresponding dependences of the theoretical quantities $\gamma_c^2(R_c)^{\text{sh}}$ and HF_0^{sh} calculated by means of the many-particle shell model. However, if such a comparison is made, it must be borne in mind that $\gamma_c^2(R_c)^{\text{exp}}$ (14) are consistently defined in the region of values of R_c in which the α particle and the daughter nucleus are fully formed (cluster region). In contrast, the theoretical reduced widths $\gamma_c^2(R_c)^{\text{sh}}$ can be correctly calculated in the region of strong overlapping of the α-decay fragments, where they fuse into the parent nucleus, losing their individuality (shell region).

Since the cluster and shell regions do not overlap, it is impossible to choose a single value of R_c for which $\gamma_c^2(R_c)^{\text{exp}}$ and $\gamma_c^2(R_c)^{\text{sh}}$ are simultaneously correctly defined. Therefore, the prescriptions usually employed in R-matrix theory,[1,3] which select a radius R_c lying in the cluster region

(see above), do explain the relative (with respect to Z, N, and the α-transition type) behavior of $\gamma_c^2(R_c)^{\text{exp}}$ but do not make it possible to reproduce their absolute values on account of the unphysical extrapolation of $\gamma_c^2(R_c)^{\text{sh}}$ beyond the shell region.

To solve the problem of describing the absolute and relative α-decay probabilities, it is expedient to consider an α-particle form factor ψ_c that determines the amplitude of the reduced width in the complete range of variation of the variable R and on this basis construct[15-22] a prescription for interpolating $\psi_c(R)$ between the shell and cluster regions.

2. CLUSTER AND SHELL FORM FACTORS AND SPECTROSCOPIC FACTORS OF α PARTICLES

1. Alpha-particle form factor and spectroscopic factor

We define the α-particle form factor for channel c as follows [19,20]:

$$\psi_c(R) \equiv \left\langle \hat{A}\left\{\frac{\delta(R-R')}{R} u_c^{\pi_i J_i M_i}\right\} \middle| \psi_{\sigma_i}^{\pi_i J_i M_i}\right\rangle, \qquad (16)$$

where $\psi_{\sigma_i}^{\pi_i J_i M_i}$ is the internal wave function of the parent nucleus, and u_c is the channel function

$$u_c^{\pi_i J_i M_i} = [\psi_{\sigma_f}^{\pi_f J_f M_f} \chi_\alpha Y_{LM_L}(\Omega_R)]_{J_i M_i}, \qquad (17)$$

in which χ_α is the internal wave function of the α particle, $Y_{LM_L}(\Omega_R)$ is a spherical function describing the relative motion of the α particle and the daughter nucleus, and the symbol $[\,]_{J_i M_i}$ denotes the vector coupling of the angular momenta of the daughter nucleus and the α particle. In (16), $\hat{A}$ is the operator of antisymmetrization between the nucleons of the α particle and the daughter nucleus; the symbol $\langle|\rangle$ denotes integration over the complete set of variables of the nucleus ${}_Z^A X_N$, including the modulus R'. For $R \leqslant R_1$, where the point R_1 lies in the below-barrier region to the left of the outer Coulomb turning point and is determined by the condition $G_c(R_1) \gg F_c(R_1)$ [$F_c(R)$ is the regular Coulomb function], the form factor $\psi_c(R)$ has the form

$$\psi_c(R) = \sqrt{\frac{\Gamma_c}{\hbar v_c}}\, G_c(R). \qquad (18)$$

For deep below-barrier α decay, the complete configuration space on which the function $\psi_{\sigma_i}^{\pi_i J_i M_i}$, which describes the quasistationary state of the α-decay nucleus, is defined can be divided into three regions[19,20] associated with different values of the variable R. The first region ($0 \leqslant R < R_{\text{sh}} \approx R_A$), called the shell region, corresponds to the internal region of the parent nucleus, in which the notions of the shell model with configuration mixing and a discrete single-particle basis are valid. The second region ($R_{\text{cl}} < R \leqslant R_1$) called the cluster region, corresponds to the outer surface region of the parent nucleus, where the α-decay fragments are fully formed. Finally, the third (intermediate) region ($R_{\text{sh}} < R < R_{\text{cl}}$) corresponds to the situation that is most complicated from the theoretical point of view-in this region, the notions of the shell model with a restricted basis are no longer valid, but the picture of completely formed α-decay fragments is also not yet valid. Making such a division, we can represent the exact α-particle form factor (16) in the form of the sum

$$\psi_c(R) = \psi_c^{\text{sh}}(R) + \psi_c^{\text{int}}(R) + \psi_c^{\text{cl}}(R), \qquad (19)$$

where the shell, $\psi_c^{\text{sh}}(R)$; intermediate, $\psi_c^{\text{int}}(R)$, and cluster, $\psi_c^{\text{cl}}(R)$ form factors are nonvanishing in the corresponding ranges of the variable R.

As a result, the total α-particle spectroscopic factor

$$W_c = \int_0^{R_1} \psi_c(R)^2\, dR \qquad (20)$$

can be represented[19,20] by analogy with (19) as a sum of three spectroscopic factors W_c^{sh}, W_c^{int}, and W_c^{cl}, each of which is determined by an expression of the type (20) in the corresponding region.

2. Form factor and spectroscopic factor of the α particle in the cluster region

In the cluster region, the wave function of the α-decay nucleus can be expressed[19,20] by the formula

$$\psi_{\sigma_i}^{\pi_i J_i M_i} = \sum_c \hat{A}\left\{\frac{u_c^{\pi_i J_i M_i} \psi_c^{\text{cl}}(R)}{R}\right\}, \qquad (21)$$

where, if the coupling of the α-decay channels is ignored, the cluster form factor $\psi_c^{\text{cl}}(R)$ satisfies the single-particle Schrödinger equation

$$\left\{-\frac{\hbar^2}{2M}\frac{d^2}{dR^2} + \frac{\hbar^2 L(L+1)}{2MR^2} + V_{\alpha A}^{\text{Coul}}(R) + V_{\alpha A}^{\text{nuc}}(R) - Q_c\right\}\psi_c^{\text{cl}}(R) = 0 \qquad (22)$$

with the boundary condition

$$\psi_c^{\text{cl}}(R) \xrightarrow[R \to R_1]{} \sqrt{\frac{\Gamma_c k_c}{2Q_c}}\, G_c(R). \qquad (23)$$

In (22), $V_{\alpha A}^{\text{Coul}}(R)$ and $V_{\alpha A}^{\text{cl}}(R)$ are the Coulomb and nuclear potentials of the α-particle interaction with the daughter nucleus. If in (23) we use the experimental value Γ_c^{exp}, then, integrating Eq. (22) from the point R_1 to $R = R_{\text{cl}}$, we can calculate the form factor $\psi_c^{\text{cl}}(R)$ and the cluster spectroscopic factor W_c^{cl}.

In the calculations of $\psi_c^{\text{cl}}(R)$ and W_c^{cl} below, we take for $V_{\alpha A}^{\text{nuc}}(R)$ the real part of the phenomenological optical potential of Ref. 35, which describes well[32,33] the interaction of α particles with nuclei at deep below-barrier energies[34]:

$$V_{\alpha A}^{\text{nuc}}(R) = V_0\,(1 + \exp[(R - R_A)/a])^{-1}, \qquad (24)$$

where $V_0 = -177.3$ MeV, $R_A = 1.34A^{1/3}$F, $a = 0.57$ F.

The quantity R_{cl} (measured in fermis) is chosen in the form

$$R_{\text{cl}} = (1.25\, A^{1/3} + 1.3) \qquad (25)$$

in accordance with the ideas considered in detail in Ref. 4 (Chap. 5).

3. Cluster form factors and spectroscopic factors with allowance for coupling of the different α-decay channels

In the calculation of the cluster spectroscopic factors for α transitions in spherical and, especially, deformed nuclei, we encounter the problem of taking into account the polarizability of the daughter nucleus; in a first approximation, this can be reduced to taking into account the coupling of the channels of α decay to the levels of collective nature in the excitation spectrum of the daughter nucleus. Such a

problem has been solved in a number of studies [36,37] in connection with the determination of the relative probabilities of α decay to vibrational and rotational states of the daughter nucleus. All these calculations were made using only the nonspherical Coulomb potential, the nuclear interaction of the α particles with the daughter nucleus being taken into account effectively by the specification of the boundary conditions on the surface of the nucleus.

In the general case, Eq. (22) for the cluster form factor $\psi_c^{\rm cl}(R)$ becomes a system of coupled equations when allowance is made for the channel coupling.[36,37] For spherical nuclei, only the coupling of the strongly collectivized vibrational states is important, and this can be taken into account in the framework of the weak-coupling approximation.[38] For deformed nuclei, it is also necessary to take into account the coupling of the rotational states in the strong-coupling approximation.[38]

The calculations of $W_c^{\rm cl}$ made in Ref. 39 for spherical even–even nuclei showed that if the excitation energy E_{2+} of the collective 2^+ level in the daughter nuclei is greater than 450 keV, then the inclusion of channel coupling leads to values of $W_c^{\rm cl}$ close to those obtained without allowance for channel coupling. But for daughter nuclei with $E_{2+} < 450$ keV allowance for channel coupling leads to an appreciable (up to three times for $W_{L=0}^{\rm cl}$ and up to ten times for $W_{L=2}^{\rm cl}$) decrease of the cluster spectroscopic factors.

The inclusion of channel coupling for α decay to rotational states of even–even deformed nuclei leads to similar results[40]—the cluster spectroscopic factors $W_L^{\rm cl}$ are reduced compared with the values of $W_L^{\rm cl}$ calculated under the assumption that there is no deformation and channel coupling by factors 2–4 for $L=0$ and 5–7 for $L=2$.

For the classification of the α transitions given below, we shall use the values of $W_L^{\rm cl}$ calculated without allowance for the channel coupling. For a detailed analysis of particular α transitions, it is necessary to consider the spectroscopic factors obtained with inclusion of channel coupling.

4. Alpha-particle form factor in the shell region

To explain the influence of the structure of the parent and daughter nuclei on the α-transition probabilities, it is natural to use the shell model, whose successes in describing the ground and excited states of nuclei, and also the probabilities of various transitions between them, are well known.[6,38]

The α-particle shell form factor for spherical nuclei in the j–j coupling scheme can be represented in the form[19,20]

$$\psi_c^{\rm sh}(R) = \sum_{\substack{P_i N_i \\ P_f N_f}} \left(\frac{A}{A-4}\right)^{N_0/2} (-1)^{N_0} (\hat{J}_{P_i}\hat{J}_{N_i}\hat{J}_f\hat{L}\hat{J}_P\hat{J}_N\hat{j}_1\hat{j}_2\hat{j}_3\hat{j}_4)^{1/2} \times \begin{Bmatrix} J_{P_f} & J_{N_f} & J_f \\ J_P & J_N & L \\ J_{P_i} & J_{N_i} & J_i \end{Bmatrix} \begin{Bmatrix} l_1 & 1/2 & j_1 \\ l_2 & 1/2 & j_2 \\ J_P & 0 & J_P \end{Bmatrix} \begin{Bmatrix} l_3 & 1/2 & j_3 \\ l_4 & 1/2 & j_4 \\ J_N & 0 & J_N \end{Bmatrix} \times \sqrt{2-\delta_{j_1 j_2}}\sqrt{2-\delta_{j_3 j_4}}\, B_{PNL}(R)\, A_{P_i N_i} A^*_{P_f N_f} G_P G_N, \quad (26)$$

where $A_{P_iN_i}$ and $A_{P_fN_f}$ are the configuration mixing coefficients in the parent and daughter nuclei, respectively, G_P and G_N are the two-particle proton and neutron coefficients of fractional parentage, $\hat{J} = 2J+1$, $\{...\}$ is the 9_j symbol, and the factor $(A/(A-4))^{N_0/2}$ is related to the elimination of the center-of-mass motion of the parent nucleus, with N_0 equal to the principal oscillator quantum number of the separated configuration of four nucleons forming the α particle. In Eq. (26), the function $B_{PNL}(R)$ is determined by[19]

$$B_{PNL}(R) = R \int D\, d\xi_1\, d\xi_2\, d\xi_3\, d\Omega_R \chi_\alpha(\xi_1, \xi_2, \xi_3) \times \prod_{k=1}^{4} R_{j_k}(r_k) [[Y_{l_1}(\Omega_{r_1}) Y_{l_2}(\Omega_{r_2})]^*_{J_P} [Y_{l_3}(\Omega_{r_3}) Y_{l_4}(\Omega_{r_4})]^*_{J_N}]_{LM}, \quad (27)$$

where $R_{j_k}(r_k)$ is the radial single-particle shell function for the state $j = nlj$, $\chi_\alpha(\xi_1, \xi_2, \xi_3)$ is the internal radial wave function of the α particle, and D is the Jacobian corresponding to the transition from the variables $\mathbf{r}_1$, $\mathbf{r}_2$, $\mathbf{r}_3$, $\mathbf{r}_4$ to the variables ξ_1, ξ_2, ξ_3, $\mathbf{R}$.

5. Nucleon pairing effects and classification of α transitions

The importance of taking into account pairing correlations when considering the absolute α-decay probabilities was first pointed out in Ref. 41, where for favored α transitions in deformed nuclei the superfluid nuclear model[6] was used to obtain enhancement factors (10^3–10^4) and justify the classification of α transitions in accordance with the degree to which they are favored. In Ref. 42, the superfluid model was used to calculate the α-decay widths of deformed nuclei in the framework of the R-matrix approach.

The need to take into account superfluid correlations in order to understand the relative behavior of the α-decay widths in spherical nuclei was demonstrated in Ref. 12 for the example of the polonium isotopes. It was shown later[17–19] that the effects of the superfluid correlations in spherical nuclei also lead to large values of the enhancement coefficients (up to 10^3) of the α-particle spectroscopic factors, and this makes it possible to explain the classification of the α transitions in these nuclei too. The use of the theory of finite Fermi systems[45] in Refs. 19, 43, and 44 led to the finding of an appreciable (up to 10^2) enhancement of the probabilities of favored α transitions in nearly magic nuclei (of the type "magic ± 2 nucleons") due to pairing effects; this was much larger than the analogous enhancement obtained earlier in Ref. 13. We note that the existence of a large pairing enhancement for the probability of the 0^+–0^+ alpha transition in the ^{212}Po nucleus was later confirmed in Ref. 46.

It is natural to consider the reason for such a strong influence of pairing correlations on the shell spectroscopic factors of the α particles. It is convenient to give the following treatment for the example of favored 0^+–0^+ alpha transitions in spherical even–even nuclei. In this case, $J_i = J_{P_i} = J_{N_i} = J_f = J_{P_f} = J_{N_f} = J_P = J_N = L = 0$, $j_1 = j_2$, $j_3 = j_4$, and the expression (26) for the shell form factor simplifies appreciably:

$$\psi_c^{\rm sh}(R) = \left(\frac{A}{A-4}\right)^{N_0/2} (-1)^{N_0} \sum_{j_1 j_3} G_{j_1} G_{j_3} B_{j_1 j_3 0}(R). \quad (28)$$

The form factor $B_{j_1 j_3 0}(R)$, determined by (27) for $J_p = J_N = L = 0$, has phase factor $(-1)^{l_1+l_3}$. At the same time, the two-proton coefficient of fractional parentage G_{j_1}, calculated in the superfluid model, has the form

$$G_{j_1} = \frac{\hat{j}_1}{2} u_{j_1}^f v_{j_1}^i (-1)^{l_1}, \quad (29)$$

where u_j, v_j are the positive-definite coefficients of the Bogolyubov u–v transformation[6] for the parent (superscript i) or daughter (superscript f) nucleus. Since the form factors $B_{j_1 j_3 0}$ and the product of the coefficients of fractional parentage G_{j_1} and G_{j_3} are completely in phase, the sum over j_1 and j_3 in (28) is coherent. This leads to a pronounced increase of the amplitude of the form factor $\psi_c^{\rm sh}(R)$ (28) compared with the amplitude of the analogous form factor $\psi_{c0}^{\rm ch}(R)$ calculated on the basis of the simple shell model, when there is only one term in the sum (28).

An analogous situation also arises for nuclei of the "magic ± 2 nucleons" type, for which the coefficients of fractional parentage G_{j_1} and G_{j_3} (Refs. 43 and 44) also have phase factors $(-1)^{l_1}$ and $(-1)^{l_3}$.

The physical reason for the pairing enhancement of the α-particle form-factor amplitudes for favored 0^+–0^+ transitions in spherical and deformed nuclei is that the pairs of identical nucleons in both the α particles and the Cooper pairs of the nuclei are in the singlet 1s' state of relative motion.

To characterize the effects of the pairing enhancement quantitatively, it is convenient to introduce the α-particle shell spectroscopic factor $W_c^{\rm sh}$ determined by Eq. (20) in terms of the shell form factor $\psi_c^{\rm sh}(R)$. Then for the favored 0^+–0^+ alpha transition the spectroscopic factor $W_c^{\rm sh}$ calculated with allowance for the pairing correlations can be expressed in terms of the factor $W_{00}^{\rm sh}$ obtained on the basis of the simple shell model:

$$W_0^{\rm sh} = k_P k_N W_{00}^{\rm sh}, \tag{30}$$

where k_P and k_N are the enhancement coefficients associated with the proton and neutron subsystems, respectively.

The calculations made in Refs. 17–19, 43, and 44 showed that for spherical nuclei with $84 \leqslant N \leqslant 130$ the values of k_P and k_N vary in the interval $10 \leqslant k_P \leqslant 30$ and $4 \leqslant k_N \leqslant 50$, respectively.

For α transitions in odd and odd–odd nuclei with selection rules $J_i = J_f$, $J_{P_i} = J_{P_f}$, $J_{N_i} = J_{N_f}$, $J_P = J_N = L = 0$, when the α particle is formed from paired pairs of protons and neutrons, the α-particle spectroscopic factor $W_0^{\rm sh}$ can be represented similarly in the form (30), but in this case the coefficients k_P and k_N are somewhat smaller, owing to the influence of the "blocking" effect.[6,19] such transitions are also favored.

In the case of α transitions for which only a proton (respectively, neutron) pair is formed in the state $J_P = 0$ (respectively, $J_N = 0$), enhancement by virtue of the pairing correlations occurs only in the proton (respectively, neutron) subsystem, and its scale is determined by the factor k_P (respectively, k_N). The hindrance factors HF_0 (33)–(37) for such α transitions must have the scale of the coefficients k_P and k_N, respectively. It is natural to call these "semifavored transitions."

Finally, for α transitions in which the neutron and proton pairs are broken and have quantum numbers $J_P \neq 0$, $J_N \neq 0$, the spectroscopic factor $W_0^{\rm sh}$ is not subject to pairing enhancement. For such α transitions, which are called unfavored, one can expect estimates of the hindrance factors of the form $\mathrm{HF}_0 \approx k_P k_N$.

Thus, allowance for the influence of the pairing correlations in the framework of the shell model makes it possible in a natural manner not only to justify the classification of the α transitions in accordance with the degree to which they are favored but also, as will be shown below, to explain the hierarchy of values of the absolute α-decay widths.

3. CLASSIFICATION OF ALPHA TRANSITIONS IN THE NON-*R*-MATRIX SCHEME

1. Cluster spectroscopic factors and hindrance factors

To analyze the experimental data on α decay, we use the experimental cluster spectroscopic factors $W_C^{\rm cl}$.[19,20] We can express $W_c^{\rm cl}$ in terms of the reduced width $\gamma_c^2(R)$ by means of Eqs. (15) and (20) in the form

$$W_c^{\rm cl} = \int_{R_{\rm cl}}^{R_1} R\gamma_c^2(R)\, dR. \tag{31}$$

By virtue of the integral definition (31), $W_c^{\rm cl}$ is much less sensitive to variation of the parameter $R_{\rm cl}$ than $\gamma_c^2(R_c)$ is to variation of the channel radius R_c. The use of $W_c^{\rm cl}$ gives a particular advantage compared with $\gamma_c^2(R_c)$ in the case of strong coupling between the different α-decay channels (see Sec. 2.3), when the α-particle form factor $\psi_c^{\rm cl}(R)$ and, with it, the amplitude of the reduced width $\gamma_c(R)$ have an irregular nature.[39,40] At the same time, comparison of the value of $W_c^{\rm cl}$ with unity, which is the limiting value of the spectroscopic factor in the single-particle model, enables one to decide whether or not quasimolecular α-particle levels are present in the nuclei. Using the values of $W_c^{\rm cl}$ for the investigated α transition and the corresponding values of $W_0^{\rm cl}$ for the favored α transitions, we can introduce by analogy with (10)–(13) the hindrance factors HF_L:

$$\mathrm{HF}_L(\mathrm{e.e}) = W_0^{\rm cl}(\mathrm{e.e})/W_c^{\rm cl}(\mathrm{e.e}); \tag{32}$$

$$\mathrm{HF}_L^N(\mathrm{e.o}) = W_0^{\rm cl}(\mathrm{e.o}-1)/W_c^{\rm cl}(\mathrm{e.o}); \tag{33}$$

$$\mathrm{HF}_L^Z(\mathrm{o.e}) = W_0^{\rm cl}(\mathrm{o}-1.\mathrm{e})/W_c^{\rm cl}(\mathrm{o.e}); \tag{34}$$

$$\mathrm{HF}_L^N(\mathrm{o.o}) = W_c^{\rm cl}(\mathrm{o.o}-1)/W_c^{\rm cl}(\mathrm{o.o}); \tag{35}$$

$$\mathrm{HF}_L^Z(\mathrm{o.o})\, W_0^{\rm cl}(\mathrm{o}-1.\mathrm{o})/W_c^{\rm cl}(\mathrm{o.o}); \tag{36}$$

$$\mathrm{HF}_L^{Z,N}(\mathrm{o.o}) = W_0^{\rm cl}(\mathrm{o}-1.\mathrm{o}-1)/W_c^{\rm cl}(\mathrm{o.o}); \tag{37}$$

In contrast to the traditionally employed expressions (10)–(13), the definitions (32)–(37) require, on the one hand, the use of a minimal number of experimental data and, on the other, match better the concepts of the shell model with allowance for pairing effects.

In the present work, we have calculated the values of $W_c^{\rm cl}$ and the corresponding hindrance factors for known α transitions of a large group of nuclides with $51 \leqslant Z \leqslant 90$ and $54 \leqslant N \leqslant 130$, including mainly spherical nuclei. In addition, for a number of the analyzed α transitions we have calculated the shell spectroscopic factors $W_c^{\rm sh}$ in accordance with Eqs. (26) and (27) with allowance for the pairing effects and configuration mixing. We give below a detailed analysis of the behavior of $W_c^{\rm cl}$ and $W_c^{\rm sh}$ for the different types of α transition and a comparison of them.

Figure 3 gives the values of $W_0^{\rm cl}$ for α transitions selected in accordance with the following principle. If the nuclide has several α transitions, only the largest value of $W_0^{\rm cl}$ for one of these transitions is given. But if for a nuclide only one α transition is observed, then the value of $W_0^{\rm cl}$ for this transition is given. In Fig. 3, isotones with $N = 127$, for which there are no favored α transitions, are not represented. It can

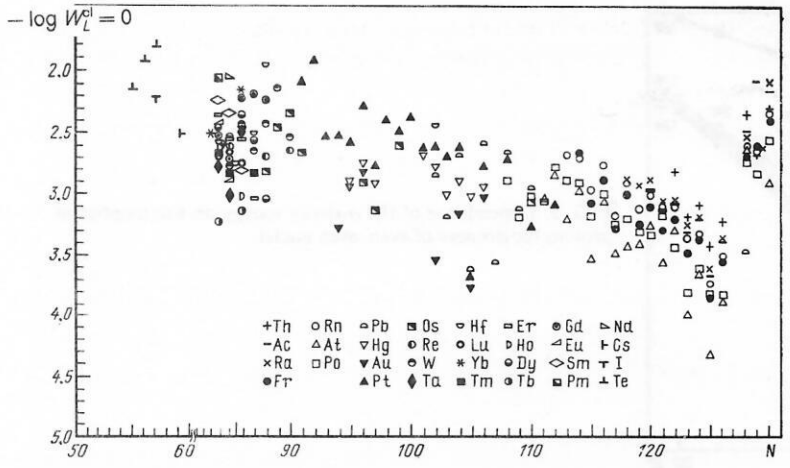

FIG. 3. The cluster spectroscopic factor for favored α transitions as a function of the number of neutrons.

be seen from Fig. 3 that for all the considered α transitions the values of W_0^{cl} are less than 10^{-2}. This fact indicates the absence in heavy nuclei of quasimolecular α-cluster levels and is in agreement with the nondetection of giant resonances in the α-particle strength function obtained from (n, α) reactions on resonance neutrons.[19,34]

2. Favored α transitions in even–even nuclei

Figure 4a gives values of W_0^{cl} for the best studied favored α transitions between the ground states of even–even nuclei; these provide the basis for the classification of all types of α transition. It can be seen that, as functions of N, the values of W_0^{cl} are grouped in a narrow strip with a spread of not more than a factor 3 from the weighted mean.[47] With decrease in the number of neutrons in the region between the "magic" numbers $N = 126$ and $N = 82$ the values of W_0^{cl} increase systematically. A significant deviation from this tendency occurs in the region $102 \leqslant N \leqslant 112$ for the isotopes of polonium, lead, and platinum. It may be due to the significant change in not only the shape[48–51] but also the parameters of the self-consistent potential in these isotopes compared with the analogous β-stable isotopes. This is indicated by the behavior of the values of $\Delta Q_\alpha(N) = Q_\alpha(Z = 84, N) - Q_\alpha(Z = 82, N)$, shown in the insert to Fig. 5. Indeed, ΔQ_α decreases from $\Delta Q_\alpha = 4.9$–3.3 MeV for $N = 122$–126 to $\Delta Q_\alpha = 1.9$–1.6 MeV for $N = 108$–112. These last values of ΔQ_α are comparable with the values of ΔQ_α characteristic of nonmagic nuclei. For example, on the transition from $Z = 76$ to $Z = 78$ for the isotopes with N equal to 108, 110, 112, 116 the values of ΔQ_α lie in the interval 1.0–1.2 MeV. The behavior of $Q_\alpha(Z)$ noted above indicates that when there is an appreciable neutron deficit the proton number $Z = 82$ ceases to be magic.

Returning to the analysis of the cluster spectroscopic factors, we note that in the region $N \geqslant 132$ the values of $W_0^{cl}(N)$ for each element are approximately constant, whereas in the region $126 \leqslant N \leqslant 130$ a decrease of N is accompanied by a decrease in the values of W_0^{cl}, this terminating with an abrupt change by up to an order of magnitude in the values of W_0^{cl} on the transition from $N = 128$ to the magic number $N = 126$. It is by this abrupt change that one can explain the appearance of two branches in the empirical dependence $\log T_{1/2}^{\alpha}(Q_\alpha)$ for each element (see Fig. 2a). A similar decrease of W_0^{cl} is observed on the transition from $N = 86$ to $N = 84$ (Fig. 4a).

By analogy with the situation in the neighborhood of $N = 126$, one can expect an abrupt change in the values of

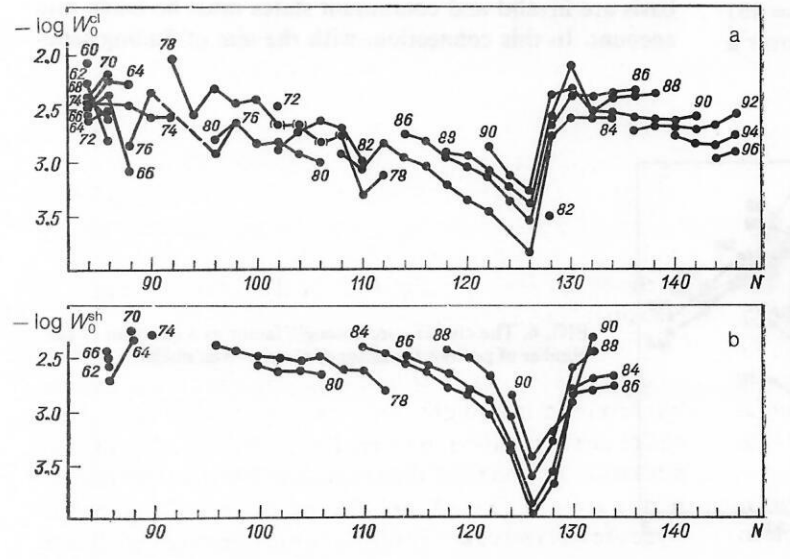

FIG. 4. The cluster spectroscopic factor for favored α transitions of even–even nuclei as a function of the number of neutrons: a) experiment; b) theory.

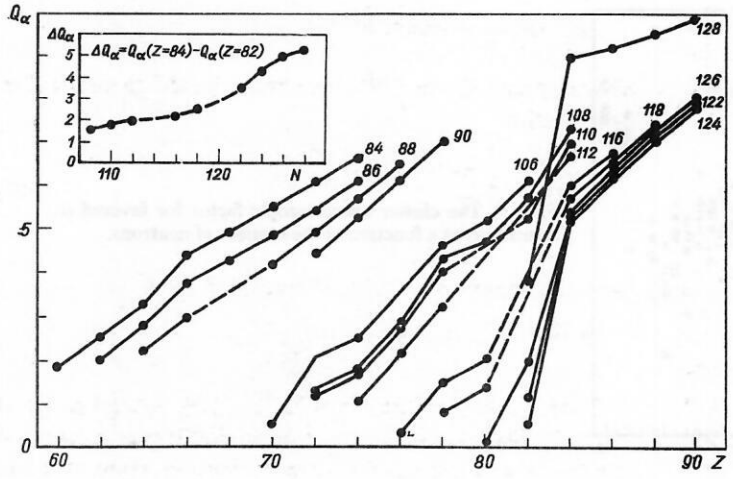

FIG. 5. Dependence of the α-decay energy on the number of protons for isotones of even–even nuclei.

W_0^{cl} on the transition from $N = 84$ to the magic number $N = 82$. Unfortunately, experimental observation of this abrupt change is difficult on account of the strong decrease in the values of Q_α for the isotones with $N = 82$.

Figure 6 gives the dependence $W_0^{cl}(Z)$ for favored α transitions in even–even nuclei. In the region $Z \geqslant 90$, the values of $W_0^{cl}(Z)$ decrease systematically with increasing Z. This tendency goes over into the opposite one for nuclei with $114 \leqslant N \leqslant 128$, i.e., the value of W_0^{cl} decreases with decreasing Z in the region $84 \leqslant Z \leqslant 90$. On the transition from $Z = 84$ to the magic number $Z = 82$, a sharp change is observed in the values of $W_0^{cl}(Z)$, which decrease by seven times at $N = 128$. It can be seen that there is a complete analogy with the abrupt change in the dependence $W_0^{cl}(N)$ on the transition from $N = 128$ to $N = 126$ (Fig. 4a). However, for $N = 108$ the transition from $Z = 84$ to $Z = 82$ is accompanied by an increase of W_0^{cl} by 1.8 times, and this may also be due to disappearance of the magic gap for $Z = 82$ and $N \leqslant 112$.

For the nuclei with $52 \leqslant Z \leqslant 80$ and $56 \leqslant N \leqslant 110$ (see Fig. 6 and Table IV) we observe a growth in the values of $W_0^{cl}(Z)$ with decreasing Z analogous to the growth of $W_0^{cl}(N)$ when the number of neutrons decreases from $N = 126$ to $N = 86$.

In the considered regions of Z and N we find the recently studied[52] doubly magic nucleus ^{146}Gd. The absence of a clear minimum in the dependence $W_0^{cl}(Z)$ at $Z = 64$ (there is a weak minimum for $N = 84$ and a maximum for $N = 86$) indicates that the proton system ceases to be magic over a small range of variation of the number of neutrons (from $N = 82$ to $N = 86$).

The features that we have considered above in the behavior of the cluster spectroscopic factor W_0^{cl} are well correlated with the behavior of the reduced α-decay widths $\gamma_c^2(R_c)^{exp}$ if the channel radius R_c is chosen appropriately.[7,8,53] In Fig. 2b we give, using the same scale as for the dependence $\log T_{\frac{1}{2}}^{\alpha}(Q_\alpha)$, the values of $\log W_0^{cl}(Q_\alpha)$ for the corresponding (see Fig. 2a) favored α transitions in even–even isotopes. Comparison of Figs. 2a and 2b shows that on a scale for which the dependence $\log T_{\frac{1}{2}}^{\alpha}(Q_\alpha)$ is represented by a straight line the variations in the values of $\log W_0^{cl}(Q_\alpha)$ can be hardly noted, whereas in fact they change by up to 30 times (see Fig. 4a). This must be borne in mind when one is interpreting α-decay data on the basis of the Geiger–Nuttall law.

The question arises of the extent to which the many-particle theory of α decay is capable of explaining the features established above in the behavior of the cluster spectroscopic factors W_0^{cl}. To answer this question adequately, it is necessary to obtain theoretically the α-particle form factor $\psi_c(R)$ in the complete range of variation of the variable R, i.e., to have a method of passing correctly from the shell to the cluster region. Unfortunately, at the present time it is not possible to calculate the form factor in the intermediate region, where the concepts of the shell model with a discrete basis are invalid and continuum states must be taken into account. In this connection, with the aim of finding semi-

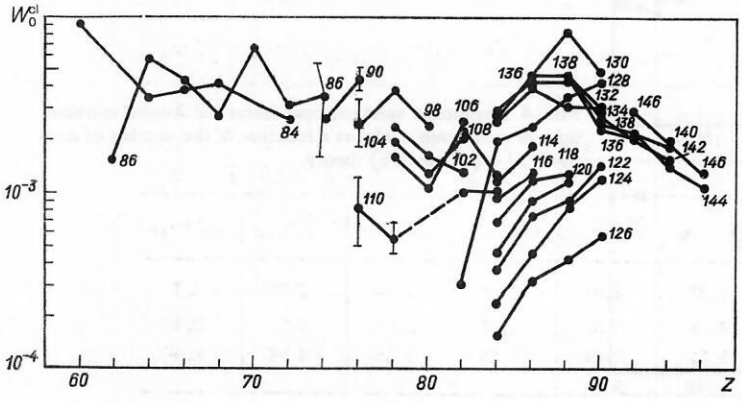

FIG. 6. The cluster spectroscopic factor as a function of the number of protons for isotones of even–even nuclei.

phenomenological prescriptions for interpolating between the shell and cluster regions, it is helpful to compare the cluster spectroscopic factors W_0^{cl} and the corresponding factors W_0^{sh} calculated on the basis of the shell model with allowance for pairing correlations.

Figure 4b gives the values of $W_0^{sh}(N)$ calculated in accordance with Eqs. (20) and (26)–(29) by means of the technique developed in Refs. 17–19 and 44 for favored α transitions in even–even nuclei. Comparison of this figure with Fig. 4a shows that overall the values of $W_0^{sh}(N, Z)$ satisfactorily reproduce the absolute values and the behavior of W_0^{cl} as a function of N and Z. The proximity of the W_0^{sh} and W_0^{cl} values appears particularly significant if one bears in mind that they were obtained independently without the use of adjustable parameters. On the basis of this result, we can, for the interpolation between the shell and cluster regions, propose the following semiphenomenological method, which with regard to the α-particle form factor is of an integral nature:

$$W_c^{cl} \approx W_c^{sh}. \tag{38}$$

The relation (38) makes it possible to calculate theoretically the absolute probabilities of the α transitions. For this, we use the rigorous formula for the α width[19,20]:

$$\Gamma_c = \Gamma_c^{s.p} \frac{W_c^{cl}}{W_c^{s.p}}, \tag{39}$$

where $\Gamma_c^{s.p}$ and $W_c^{s.p}$ are the widths and cluster spectroscopic factor of the single-particle α-decay state; they can be readily calculated by integrating the single-particle Schrödinger equation (22) in the complete region $0 \leqslant R \leqslant R_1$ for the wave function $\psi_c^{s.p}(R)$ with the boundary conditions (23) and

$$\psi_c^{s.p}(R) \xrightarrow[R\to 0]{} \text{const } R^{(L+1)}.$$

Substituting (38) in (39), we obtain for the theoretical α-decay width

$$\Gamma_c^{th} = \Gamma_c^{s.p} \frac{W_0^{sh}}{W_0^{s.p}}. \tag{40}$$

Note that comparison of (39) and (49) gives

$$\Gamma_c^{exp}/\Gamma_c^{th} = W_c^{cl}/W_c^{sh}.$$

In Table I, we give the ratios $\Gamma_c^{exp}/\Gamma_c^{th}$ for a large group of favored α transitions in even–even nuclei. It can be seen that the theoretical formula (40) reproduces the absolute values of the experimental α-decay widths (and, therefore, their dependence on N and Z) up to a factor that is basically at the level 3. Larger deviations are observed for the nuclei with N equal to 128 and 130, for which the existing theoretical schemes cannot, apparently, reproduce qualitatively the jump in the values of W_0^{cl} on the transition through the magic neutron number $N = 126$. At the same time, the deviations of Γ_c^{th} from Γ_c^{exp} reaching a factor 4 for the ^{186}Os and ^{194}Po nuclei could be due either to the appearance of significant equilibrium deformations (^{186}Os) or rearrangement of the self-consistent field (^{194}Po), as a result of which the proton number $Z = 82$ ceases to be magic in the region $N \lesssim 110$ (see the discussion above). The successful use of the relation (38) for the explanation of the absolute and relative probabilities of favored α transitions in even–even nuclei—the reference transitions for the classification of the α-decay width—creates a promising basis for the use of the condition (38) in the analysis of all other α transitions.

TABLE I. Comparison of experimental and theoretical spectroscopic factors and α-decay widths for favored α transitions in even–even nuclei.

Element	$^{148}_{62}Sm_{86}$	$^{150}_{64}Gd_{86}$	$^{152}_{64}Gd_{88}$	$^{152}_{86}Dy_{86}$	$^{154}_{68}Er_{86}$	$^{174}_{72}Hf_{102}$	$^{164}_{74}W_{90}$	$^{186}_{76}Os_{110}$	$^{180}_{80}Hg_{100}$	$^{182}_{80}Hg_{102}$	$^{184}_{80}Hg_{104}$
$-\log W_0^{cl}$	2,78	2,23	2,25	2,4	2,57	2,46	2,56	~ 3,05	~ 2,81	2,8	2,9
$-\log W_0^{sh}$	2,54	2,54	2,31	2,52	2,52	2,96	2,28	3,68	2,51	2,52	2,54
Γ^{exp}/Γ^{th}	0,58	2,04	1,15	1,32	0,89	3,16	0,52	~ 4,27	~ 0,5	0,52	0,44
Element	$^{186}_{80}Hg_{106}$	$^{194}_{84}Po_{110}$	$^{196}_{84}Po_{112}$	$^{198}_{84}Po_{114}$	$^{200}_{84}Po_{116}$	$^{202}_{84}Po_{118}$	$^{204}_{84}Po_{120}$	$^{206}_{84}Po_{122}$	$^{208}_{84}Po_{124}$	$^{210}_{84}Po_{126}$	$^{212}_{84}Po_{128}$
$-\log W_0^{cl}$	2,97	3,03	2,8	2,93	3,03	3,21	3,33	3,44	3,62	3,83	2,72
$-\log W_0^{sh}$	2,6	2,39	2,43	2,55	2,59	2,76	2,8	3,03	3,34	4	3,68
Γ^{exp}/Γ^{th}	0,43	0,23	0,43	0,42	0,36	0,35	0,3	0,39	0,52	1,48	9,12
Element	$^{214}_{84}Po_{130}$	$^{200}_{86}Rn_{114}$	$^{202}_{86}Rn_{116}$	$^{204}_{86}Rn_{118}$	$^{206}_{86}Rn_{120}$	$^{208}_{86}Rn_{122}$	$^{210}_{86}Rn_{124}$	$^{212}_{86}Rn_{126}$	$^{214}_{86}Rn_{128}$	$^{216}_{86}Rn_{130}$	$^{206}_{88}Ra_{118}$
$-\log W_0^{cl}$	2,56	2,72	2,78	2,92	3,02	3,11	3,35	3,53	2,63	2,34	2,91
$-\log W_0^{sh}$	2,8	2,51	2,59	2,66	2,8	2,9	3,32	3,89	3,58	2,84	2,43
Γ^{exp}/Γ^{th}	1,74	0,62	0,65	0,55	0,6	0,6	0,93	2,29	8,9	3,16	0,33
Element	$^{208}_{88}Ra_{120}$	$^{210}_{88}Ra_{122}$	$^{212}_{88}Ra_{124}$	$^{214}_{88}Ra_{126}$	$^{216}_{88}Ra_{128}$	$^{218}_{88}Ra_{130}$	$^{214}_{90}Th_{124}$	$^{216}_{90}Th_{126}$	$^{218}_{90}Th_{128}$	$^{220}_{90}Th_{130}$	
$-\log W_0^{cl}$	2,91	3,06	3,21	3,38	2,55	2,08	3,11	3,25	2,36	2,3	
$-\log W_0^{sh}$	2,52	2,67	3,05	3,6	3,28	2,59	2,85	3,42	3,2	2,91	
Γ^{exp}/Γ^{th}	0,41	0,41	0,69	1,66	5,37	3,24	0,55	1,48	6,92	4,07	

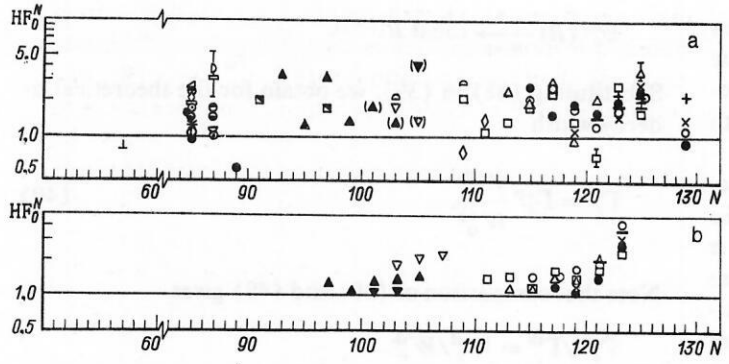

FIG. 7. Neutron hindrance factors as functions of the number of neutrons: a) experiment; b) theory; for the notation, see Fig. 3.

3. Favored α transitions in odd and odd–odd nuclei

In Figs. 7a and 8a we give the neutron and proton hindrance factors HF_0 (33)–(37) for α transitions in the odd and odd–odd nuclei for which the necessary experimental data are available. Among all the known α transitions in each isotope we have selected just the one α transition with the maximal value of W_0^{cl}. Only for a number of the isotopes of astatine, francium, and actinium, for which in each case two favored α transitions are observed,[54,55] are the hindrance factors given in Figs. 7a and 8a with allowance for the total W_0^{cl} values for these transitions. In the cases when the spins and parities of the parent and daughter nuclei have been established, $J_i^{\pi_i} = J_f^{\pi_f}$, for the analyzed α transitions, a result that corresponds to the condition for an α transition in odd and odd–odd nuclei to be favored.

As can be seen from Figs. 7a and 8a, respectively, the neutron and proton hindrance factors HF_0^N and HF_0^Z have values that do not differ greatly for isotopes with different Z and for all investigated cases do not exceed 4. We note that on the transition through the magic numbers $N = 126$ and $Z = 82$ no abrupt changes in the values of HF_0^N and HF_0^Z occur. It is interesting to note that for a large group of odd and odd–odd nuclei in the range of neutron numbers $111 \leqslant N \leqslant 130$ the HF_0^Z values are grouped in a narrow band from 0.9 to 1.3. Therefore, the significantly larger hindrance factors HF_0^Z for the isotoes ^{198,210,215}At are noteworthy. For ^{198}At one can expect, by analogy with ^{200,202,210}At, ^{202,212}Fr, the existence of a second favored α transition, which is not observed experimentally. Allowance for it may significantly reduce the value of HF_0^Z and bring it into agreement with the values of the proton hindrance factors for the other nuclei in this region. In the cases of the isotopes ^{210,215}At, the experimental half-lives and α-decay fractions must apparently be determined more accurately.

In accordance with the definition of the hindrance factors HF_0^N and HF_0^Z they should not be significantly less than unity. Therefore, the appearance of signifcantly smaller hindrance factors is a clear indication of inaccuracy of the corresponding experimental data.

We note that the hindrance factor $HF_L^{Z,N}(o.o)$ determined by Eq. (37) can be expressed in terms of a product of neutron and proton hindrance factors:

$$HF_L^{Z,N}(o.o) = HF_L^Z(o.o)\, HF_L^N(o - 1.o). \qquad (41)$$

Since the factors $HF_0^Z(o.o)$ and $HF_0^N(o - 1.o)$ have already been obtained (see Figs. 7a and 8a), the factors $HF_0^{Z,N}(o.o)$ can be examined on the basis of the data given above.

Figures 7b and 8b give the theoretical values of the neutron and proton hindrance factors obtained when the quantities W_0^{cl} in Eqs. (33)–(36) are replaced by the shell spectroscopic factors W_0^{sh} calculated on the basis of the technique of Refs. 17, 19, and 44. It can be seen that the experimental, HF_0^N, and theoretical, $(HF_0^N)^{th}$, factors agree satisfactorily for all the analyzed nuclei. It should be noted that the factors $(HF_0^N)^{th}$ reproduce the tendency for the HF_0^N to increase when the neutron number increases from $N = 115$ to $N = 125$, this being due to the transition of the state of the

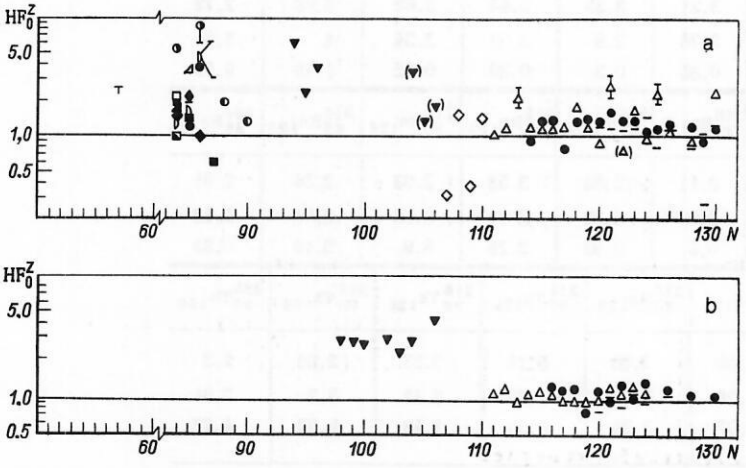

FIG. 8. Proton hindrance factors as functions of the number of neutrons: a) experiment; b) theory; for the notation, see Fig. 3.

odd neutron from the $3p_{3/2}$ subshell to the $2f_{5/2}$ and $3p_{1/2}$ subshells. At the same time, the theoretical values of the proton hindrance factors $(HF_0^Z)^{th}$ are clearly grouped in a very narrow band from 0.9 to 1.4 for all nuclides with $111 \leqslant N \leqslant 130$, and this agrees well with the behavior of the experimental HF_0^Z. Such behavior of the proton hindrance factors can be explained by the fact that for all the considered isotones the odd proton is in the $1h_{9/2}$ subshell, for which the "blocking effect"[41] is small, owing to the large spin value $j = 9/2$ of the blocked orbital. Note that in the region of nuclei with $N < 110$ the $(HF_0^Z)^{th}$ values are in reasonable agreement with the experimental HF_0^Z.

4. Semifavored α transitions

The experimental study of the α decay of the ground states of odd nuclei has revealed in a number of isotopes some α transitions corresponding to excitation energies E_f^* of the daughter nuclei less than 1 MeV. Among these α transitions, a favored transition is, as a rule, observed. In rare cases, one observes α transitions with $L = 2$ having W_0^{cl} values close to favored values. Such transitions are associated with excitation in the core of a low-lying collective 2^+ phonon.[39] All the remaining transitions correspond to cases of $J_i^{\pi_i} \neq J_f^{\pi_f}$ with $L \neq 0$ and have W_0^{cl} values less than W_0^{cl} for favored α transitions. Such transitions are semifavored (see Sec. 2.5), since the breaking of the pair of nucleons taken out of the even subsystem leads to a transition to excited states of the daughter nucleus with energies $E_f^* \geqslant 2$ MeV. The α transitions in the odd isotopes of polonium, radon, radium, and thorium with $N = 127$ provide a typical example of semifavored α decays with no enhancement in the neutron subsystem. Indeed, in this case the states of the odd neutron in the parent $(2g_{9/2})$ and daughter $(3p_{1/2}, 2f_{5/2}, 3p_{3/2}, \ldots)$ nuclei belong to different shells, and this leads to the following possible configurations of the broken neutron pair that partici-

TABLE II. Semifavored α transitions.

N	Z	E_α, keV	$T_{1/2}$	α, %	I_α for 100 α decays	$J_i^{\pi_i}$	$J_f^{\pi_f}$	L	$-\log W_L^{cl}$	HF_L
127	90	9250(10)	0.252(7) msec	100	100	$(9/2^+)$	$(1/2^-)$	0	4.80(1)	35(3)
								5	3.76(1)	3.2(2)
127	88	8697(5)	$1.56(10)\cdot10^{-3}$sec	100	95.7(10)	$(9/2^+)$	$1/2^-$	0	4.913(30)	35(3)
								5	3.873(30)	3.2(3)
	88	8167(8)	$1.56(10)\cdot10^{-3}$sec	100	1.3(5)	$(9/2^+)$	$(5/2^-)$	0	5.35(17)	95(37)
								3	4.88(17)	32(13)
	88	7879(8)	$1.56(10)\cdot10^{-3}$sec	100	3.0(5)	$(9/2^+)$	$(3/2^-)$	0	4.14(8)	5.9(11)
								3	3.67(8)	2.0(4)
127	86	8085(10)	25.0(2) msec	100	99	$(9/2^+)$	$1/2^-$	0	5.123(35)	40(4)
								5	4.043(35)	3.3(3)
	86	7550(15)	25.0(2) msec	100	1	$(9/2^+)$	$5/2^-$	0	5.519(35)	98(9)
								3	5.069(35)	35(3)
127	84	7450.6(19)	0.516(3) sec	100	98.917	$(9/2^+)$	$1/2^-$	0	5.285(25)	29(2)
								5	4.185(25)	2.3(1)
	84	6892.5(25)	0.516(3) sec	100	0.546(19)	$(9/2^+)$	$5/2^-$	0	5.685(25)	72(4)
								3	5.231(25)	25.2(15)
	84	6570.0(25)	0.516(3) sec	100	0.537(19)	$(9/2^+)$	$3/2^-$	0	4.493(25)	4.6(3)
								3	4.043(25)	1.6(1)
125	90	7524(8)	1.2(2) sec	100	40(3)	$(1/2^-)$	$(5/2^-)$	0	3.996(80)	7.7(21)
								2	3.768(80)	4.5(13)
	90	7333(10)	1.2(2) sec	100	8(3)	$(1/2^-)$	$(3/2^-)$	0	4.04(18)	8.6(40)
								2	3.82(18)	5(2)
125	88	6731(5)	2.75(15) min	80(5)	45(2)	$(1/2^-)$	$(5/2^-)$	0	4.190(41)	9.6(9)
								2	3.962(41)	5.7(6)
	88	6521(5)	2.75 (15) min	80(5)	6(1)	$(1/2^-)$	$(3/2^-)$	0	4.131(81)	8.4(16)
								2	3.903(81)	5.0(9)
125	86	5850(2)	15.0(5) h	26(1)	34(1)	$1/2^-$	$5/2^-$	0	4.333(26)	9.6(7)
								2	4.099(26)	5.6(4)
		5616(3)	15.0(5) h	26(1)	2.7(2)	$1/2^-$	$3/2^-$	0	4.280(39)	8.5(8)
								2	4.054(39)	5.0(5)
125	84	4617(5)	102(5) yr	99.74(3)	0.48(2)	$1/2^-$	$3/2^-$	0	4.428(27)	6.4(4)
								2	4.194(27)	3.7(2)
123	86	5898(3)	28.5(10) min	17(2)	0.14(2)	$5/2^-$	$(1/2^-)$	0	5.573(82)	293(57)
								2	5.346(82)	174(34)
		5887(3)	28.5(10) min	17(2)	0.22(2)	$5/2^-$	$(3/2^-)$	0	5.325(66)	166(26)
								2	5.101(66)	99(16)
121	86	6068(3)	9.27(5) min	23(2)	0.66(2)	$5/2^-$	$(3/2^-)$	0	5.033(42)	103(11)
								2	4.809(42)	61(7)
		5995(4)	9.27(25) min	23(2)	0.10(3)	$5/2^-$	$(1/2^-)$	0	5.52(14)	319(102)
								2	5.30(14)	190(61)
128	83	6623.1(6)	2.15 min	99.726(4)	83.57(4)	$(9/2^-)$	$1/2^+$	0	5.329(1)	72(1)*
								5	4.201(1)	5.4(10)*
		6278.8(6)	2.15 min	99.726(4)	16.43(4)	$(9/2^-)$	$3/2^+$	0	4.680(1)*	16(3)*
								3	4.226(1)	5.7(10)*
84	65	3967(3)	4.10(5) h	16.7(4)	99.97	$(3/2^+)$	$5/2^+$	0	3.239(36)	5.1(6)*
								2	2.969(36)	2.8(3)*
		3644(5)	4.10(5) h	16.7(4)	$3(1)\cdot10^{-2}$	$(3/2^+)$	$7/2^+$	0	4.55(15)	105(37)*
								2	4.28(15)	56(20)*
86	65	3409(5)	17.5(7) h	$9.5(15)\times\times10^{-3}$	99.9	$1/2^+$	$5/2^+$	0	3.147(71)	8(2)*
								2	2.876(71)	4.4(8)*
								0	4.208(71)	95(16)*
		3183(5)	17.5(7) h	$9.5(15)\times\times10^{-3}$	0.1	$1/2^+$	$7/2^+$	4	3.308(71)	12(2)*

Note. *Proton hindrance factors HF_L^Z; in the remaining cases, neutron hindrance factors are given.

pates in the formation of the α particle:

$$[2g_{9/2},\ 3p_{1/2}]_L;\quad [2g_{9/2},\ 2f_{5/2}]_L;\quad [2g_{9/2},\ 3p_{3/2}]_L\ \ldots$$

As can be seen from Table II, the neutron hindrance factors HF_0^N for these configurations lie in the range $5 \leqslant HF_0 \leqslant 100$.

In Table II we also give experimental data on the α decay of the odd isotopes of thorium, radium, radon, and polonium with $N = 125$, $N = 123$, and $N = 121$, for which the semifavored α transitions are associated with the following configurations of the neutron pair that is carried away:

$$[3p_{1/2},\ 2f_{5/2}]_L;[3p_{1/2},\ 3p_{3/2}]_L;[2f_{5/2},\ 3p_{1/2}]_L;[2f_{5/2},\ 3p_{3/2}]_L.$$

The hindrance factors HF_0 for these α transitions lie in the range $6 \leqslant HF_0 \leqslant 300$.

We note that semifavored α transitions without enhancement in the neutron subsystem are observed experimentally in the α decay of the odd–odd isotopes of actinium, francium, and astatine, for which the hindrance factors HF_0^N lie in approximately the same range (6–300).[55] However, detailed analysis of these α transitions is complicated by the absence of information on the spins and structure of the initial and final states.

The α transitions in the nuclei ^{211}Bi and ^{149,151}Tb provide a typical example of semifavored α transitions with hindrance in the proton subsystem. In the case of the α decay of ^{211}Bi, the states of the odd proton in the parent ($1h_{9/2}$) and daughter ($3s_{1/2}$ or $2d_{3/2}$) nuclei belong to different proton shells. Similarly, the odd proton in the isotopes ^{149}Tb and ^{151}Tb is in the states $2d_{3/2}$ and $3s_{1/2}$, respectively, but in the daughter isotopes ^{145,147}Eu it is in the states $2d_{5/2}$ and $1g_{7/2}$ for the ground and first excited levels, respectively. As can be seen from Table II, the hindrance factors HF_0^Z for these α transitions lie in the interval from 5 to 125 which is close to the interval of values obtained for the hindrance factors HF_0^Z.

Since for the majority of the semifavored α transitions considered in Table II there is information about the spin states of the parent and daughter nuclei, one can, besides the hindrance factors HF_0, also calculate the reduced hindrance factors HF_L. As can be seen from Table II, which gives the values obtained for HF_L, they lie in the range $2 \leqslant HF_L \leqslant 190$, which is close to the corresponding range $5 \leqslant HF_0^{N(Z)} \leqslant 300$ for the hindrance factors. We note that the hindrance factors HF_L are helpful in the detailed theoretical analysis of particular α transitions. But for classification purposes, especially when there is no information about the spins or parities of the states participating in the α transition, it is expedient to use the hindrance factors HF_0.

In comparing the interval of hindrance factors $HF_L^{N(Z)}$ obtained above with the theoretical estimates given in Sec. 2.5, $HF_L^{N(Z)} \simeq k_N(k_P)$, it must be borne in mind that these estimates were made in the approximation of constancy of the spectroscopic factors W_{00}^{sh} calculated in the simple shell model. However, because of the dependence of the geometrical factors and the matrix elements that determine W_{00}^{sh} on the particular configurations of the pairs of separated nucleons, this is a rough approximation, so that comparison of the proton (respectively, neutron) enhancement coefficients with the corresponding hindrance factors $HF_L^{Z(N)}$ may be only qualitative in nature. In the light of this discussion, it can be noted that the interval of values of the hindrance factors $HF_L^{N(Z)}$ agrees satisfactorily with the intervals of k_P and k_N values given in Sec. 2.5.

Unfortunately, a systematic theoretical analysis of the shell spectroscopic factors with allowance for pairing effects for semifavored α transitions has not yet been made. In Ref. 56, a comparison of favored and semifavored α transitions in isotones with $N = 125$ yielded only qualitative estimates of the neutron enhancement coefficient. And in the calculations made in Ref. 57 for ^{210}At and based on R-matrix theory, pairing correlations were not taken into account even in the analysis of the relative intensities of favored and semifavored α transitions.

It would therefore be well worthwhile making a detailed theoretical study of the hindrance factors for semifavored α transitions, particularly in the cases when reduced hindrance factors are not large, i.e., $HF_L \leqslant 6$.

In conclusion, we demonstrate the possibilities of the shell model for the description of the relative intensities of semifavored α transitions in the cases when lengthy numerical calculations are not required. On the basis of knowledge of the shell spectroscopic factors, one can expect that for each of the semifavored α transitions $9/2^+ \to 1/2^-$, $9/2^+ \to 5/2^-$, and $9/2^+ \to 3/2^-$ in different isotopes with $N = 127$ and the α transitions $1/2^- \to 5/2^-$ and $1/2^- \to 3/2^-$ in the studied isotopes with $N = 125$ the neutron hindrance factors HF_0^N must have similar values. This prediction is confirmed experimentally, since, as follows from Table II, the values of HF_0^N for these transitions lie in the ranges 29–35, 72–95, 4.6–5.9, 7.7–9.6, and 6.4–8.6, respectively.

The ratio ω of the neutron hindrance factors HF_0^N for the semifavored α transitions $5/2^- \to 3/2^-$ in the isotopes ^{207}Rn and ^{204}Rn, under the assumption that the states of the odd neutrons in the parent and daughter nuclei are pure shell states $2f_{5/2}$ and $3p_{3/2}$ and when allowance is made for Eqs. (20), (26), and (27), is equal to the inverse of the ratio of the squares of the neutron coefficients of fractional parentage G_N. For the odd neutron subsystem, the coefficients G_N are determined with good accuracy as[12]

$$G_N = \sqrt{\frac{2J_N+1}{2}}\sqrt{\frac{(\Omega_{j_i} - n_{j_i})\, n_{j_f}}{\Omega_{j_i}^2 \Omega_{j_f}^2}}, \qquad (42)$$

where n_{j_i} and n_{j_f} are the numbers of neutron pairs in the subshells $j_i = J_i$ and $j_f = J_f$ in the parent nucleus, and $\Omega_j = \hat{j}/2$ is the maximally possible number of pairs in subshell j. Then the theoretical value is $\omega = 0.5$, in good agreement with the ratio $\omega = 0.62$ of the experimental hindrance factors $HF_0^N(^{207}\text{Rn})$ and $HF_0^N(^{209}\text{Rn})$ in Table II.

The theoretical value of the ratio ω of the neutron hindrance factors HF_0^N for the semifavored α transitions $1/2^- \to 5/2^-$ in ^{211}Rn and $5/2^- \to 3/2^-$ in ^{209}Rn is found by the use of Eqs. (20), (26), (27), and (42) to be 0.062. The corresponding ratio of the experimental hindrance factors HF_0^N for these α transitions is 0.058 (see Table II).

5. Unfavored α transitions

For α decay from the ground states of nuclei to low-lying levels of the daughter nuclei ($E_f^* < 1$ MeV) unfavored α transitions can be observed only in odd–odd nuclei. At the present time, such α transitions have been found only in the

nucleus ^{210}Bi. For the α decay of isomer states, unfavored α transitions can also be observed in the case of odd ($E_i^* > 1$ MeV) and even–even ($E_i^* > 2$ MeV) nuclei, in which case Cooper pairs of nucleons are broken in the even subsystems of the parent nuclei. Typical examples of such α transitions are the transitions from the isomer state ^{212}Po^m (16^+) to the 0^+, 3^-, and 5^- levels of the nucleus ^{209}Pb.

In the case of odd–odd nuclei, one can expect that the neutron, HF_0^N, and proton, HF_0^Z, hindrance factors determined by the expressions (35) and (36), where the numerators contain W_0^{cl}(o.o − 1) and W_0^{cl}(o − 1,o) for the semifavored α transitions in the neighboring odd isotopes, must be close to the corresponding hindrance factors for the semifavored α transitions in the neighboring odd nuclei. At the same time, the hindrance factor $HF_0^{Z,N}$ for unfavored α transitions, represented in the form (41), must be close in value to the product $HF_0^Z \cdot HF_0^N$, where HF_0^Z and HF_0^N, correspond to the semifavored α transitions considered in Sec. 3.4. Then the range of variation of $HF_0^{Z,N}$ for unfavored α transitions is determined as 25–10^4. For a more accurate estimate of the lower limit of $HF_0^{Z,N}$ one can use α transitions from the ground state of ^{210}Bi(1^-) to the 2^- and 1^- levels of ^{206}Tl. These transitions are unfavored, since the states of the odd proton and odd neutron in ^{210}Bi and ^{206}Tl belong to different shells. Unfortunately, it is not possible to calculate the factor $HF_0^{Z,N}$(o.o) rigorously in accordance with the expression (37), since experimental data on the α decay of the nucleus ^{208}Pb are not available.

In this connection, one can obtain only an approximate estimate of the factor $HF_0^{Z,N}$ by using the experimental value of W_0^{cl} for ^{210}Pb and recovering the value of WW_0^{cl} for ^{208}Pb under the condition that the dependence $W_0^{cl}(N)$ for the lead isotopes is similar to the dependence $W_0^{cl}(N)$ for the isotopes of polonium, radon, radium and thorium. In this case for Pb we obtain $W_0^{cl} \approx 6 \times 10^{-5}$. Then for the transitions $1^- \to 2^-$ and $1^- \to 1^-$ in ^{210}Bi the estimates of $HF_0^{Z,N}$ lie in the range 10–20 and differ from the values of the factors $F_0^{Z,N}$ obtained on the basis of the Geiger–Nuttall law in the compilation of Ref. 5 by a factor ≈ 3. Thus, the lower limit of the range of values of the factors $HF_0^{Z,N}$ can be reduced to 10, which is close to the corresponding lower bound for the hindrance factors $HF_0^{Z(N)}$ in the case of semifavored α transitions. On the other hand, the upper limits of the ranges of values of the hindrance factors $HF_0^{Z,N}$ and $HF_0^{Z(N)}$ are also about the same, both because of the strong influence of structure hindrances on the probabilities of the semifavored α transitions and because of the experimental restrictions on the observation of weak α lines.

In Refs. 58 and 59 the shell spectroscopic factors were calculated on the basis of Eqs. (26) and (27) for the unfavored α transitions $1^- \to 2^-$ and $1^- \to 1^-$ in ^{210}Bi. The ratios of the values of the experimental cluster, W_c^{cl}, and shell, W_c^{sh}, spectroscopic factors were found to be 0.9 and 3.4, respectively, for these α transitions when pure shell states are used in the calculations. Allowance for configuration mixing in the wave functions of the parent and daugther nucleus[60,61] leads to values 0.28 and 2 for these ratios. This result indicates the possibility of theoretical description of the absolute probabilities of an unfavored α decay to within a factor 4.

It should be noted that comparison of the hindrance factors HF_0^N(e.o), HF_0^Z(e.o), and $HF_0^{Z,N}$(o.o) from the present paper with the corresponding hindrance factors F_0 (11)–(13) from Ref. 5 reveals a qualitative agreement between them. We note that the largest discrepancies between the hindrance factors HF_0 and F_0, which reach a factor 3, arise in the region $N \simeq 126$, where analysis of α-decay data on the basis of the Geiger–Nuttall law is incorrect. This fact was already pointed out in Ref. 1.

4. ANALYSIS OF EXPERIMENTAL DATA AND PREDICTIONS

Using the experience accumulated from the study of α transitions that are favored to different degrees, and using the experimental cluster spectroscopic factors, we can analyze the experimental data on α decay for a wide range of nuclei and make fairly reliable theoretical predictions. A good example of such analysis is provided by the study of the α decay of the neutron-deficient isotopes of bismuth made in Ref. 48.

1. Alpha decay of neutron-deficient isotopes of bismuth

Alpha decay of neutron-deficient isotopes of bismuth has been observed in the range of mass numbers $A = 203$–188. The corresponding experimental data were analyzed in detail in Ref. 48 (see also Sec. 5.7 in Ref. 4) on the basis of the systematics of the cluster spectroscopic factors. In Ref. 48 hypotheses about the structure of the states of the parent and daughter nuclei, and also about the nature of the α transitions connecting these states, were proposed and justified. This made it possible to predict the α fractions not only for α transitions unknown at the time of the study (1978) but also for α transitions whose experimental characteristics appeared to contradict the theory.

Table III gives experimental data on the α decay of bismuth isotopes from Ref. 62, which appeared after the publication of Ref. 48. The final column of this table gives the α-decay fractions predicted in Ref. 48, the fractions for the α transition $1/2^+ \to 1/2^+$ in the isotopes ^{191,197}Bi having been recalculated to take into account new values of E_α and $T_{1/2}$.[62] Comparison of the α fractions from Refs. 62 and 48 shows that they do not differ much; this indicates that the ideas proposed in Ref. 48 about the structure of the states connected by the α transitions in the bismuth and thallium isotopes are valid, and also reveals the predictive strength of the cluster spectroscopic factors for α-decay analysis.

2. Systematics of the characteristics of α transitions

Table IV gives experimental data for the α decay of isotopes with $52 \leqslant Z \leqslant 90$ and $84 \leqslant N \leqslant 130$. As a rule, for each of the isotopes we give in the table only the one α transition with the maximal value of W_0^{cl}, and it is only for a number of odd–odd isotopes of actinium, francium, and astatine that two favored α transitions are given for each. When several sets of experimental data were available for a particular α transition, preference was given to the results with the smallest errors. In the cases when the experimental data obtained in different studies do not overlap within comparable errors, they are both included in the table.

Table IV does not include isotopes for which there are no experimental values of $T_{1/2}$ or the α-decay fractions (provided they are significantly less than 100%).

In the majority of the considered cases, the experimen-

TABLE III. Characteristics of α transitions of bismuth isotopes with $A \leqslant 197$.

Experiment								Systematics	
A	E_α, keV	$T_{1/2}$, sec	α, %	Transition $J_i^{\pi} i - J_f^{\pi} f$	L	$-\log W_L^{cl}$	HF_L	$-\log W_L^{cl}$	α, %
197*m*	5760(20)	329(20)	>1	$1/2^+ - 1/2^+$	0	<3.81	—	>2.95	<7
195*g*	5420(5)	187(1)	0.04	$9/2^- - 9/2^-$	0	3.26	—	2.87	0.1
195*g*	5713(5)	187(1)	0.01	$9/2^- - 1/2^+$	0	5.31	—	5.46	0,007
				$9/2^- - 1/2^+$	5	4.17	—	4.32	—
195*m*	6106(5)	87(1)	<52	$1/2^+ - 1/2^+$	0	3.02	—	>2.92	<66
194	5598(5)	125(1)	0.21	$(10^-) - (10^-)$	0	3.24	1.3*	3.25	0.2
193*g*	5899(5)	69(1)	3.8	$9/2^- - 9/2^-$	0	3.12	1.4**	3.02	5
193*g*	6174(5)	69(1)	0.2	$(9/2^-) - (1/2^+)$	0	5.59	—	5.62	0.2
				$9/2^- - 1/2^+$	5	4.45	—	4.50	—
193*m*	6475(5)	~ 3.5	~ 100	$1/2^+ - 1/2^+$	0	2.81	—	>3.10	<50
192	6055(5)	39(1)	26	$(10^-) - (10^-)$	0	2.70	0.4**	2.86	18
191*g*	6311(5)	11.1(3)	59.2	$(9/2^-) - (9/2^-)$	0	2.85	1.5**	3.12	32
191*g*	6639(5)	11.1(3)	1.8	$9/2^- - 1/2^+$	0	5.64	—	5.63	1.8
				$9/2^- - 1/2^+$	5	4.52	—	4.51	—
191*m*	6876(5)	~ 0.3 ***	~ 100	$1/2^+ - (1/2^+)$	0	3.19	—	3.35	68
190	6453(5)	5.2(2)	59.9	$(10^-) - (10^-)$	0	3.06	0.3**	2.90	87

Note. $HF_0^N(^{192}Bi) = 0.7$; *corresponds to HF_0^N; **corresponds to HF_0^Z; all the experimental data are taken from Ref. 62; the values for the log W_0^{cl} systematics are given in accordance with Ref. 48; ***in Ref. 70 the value $T_{1/2} = 0.15(2)$ sec is obtained.

tal values of the cluster spectroscopic factors and the hindrance factors agree well with the general systematics of $W_0^{cl}(Z)$, $W_0^{cl}(N)$, and the hindrance factors (see Secs. 3.1–3.4), and they are also correlated with the behavior of the shell spectroscopic factors and theoretical hindrance factors. This indicates that the existing experimental data are fairly reliable for the considered cases. Below, such α transitions are not discussed. But in the cases when the values of W_0^{cl} or HF_0 deviate significantly from the systematics and disagree with the corresponding theoretical values, Table V gives predictions for the expected values of W_0^{cl}, and also in a number of cases for α, and these can serve as a basis for correction of the experimental data. In the seventh column of Table IV we give the factors W_0^{cl} used for the analysis and predictions.

We now discuss in more detail for specific nuclei the reasons for a revision of the experimental data and for making predictions of the expected W_0^{cl} values, and, in a number of cases, the α fractions. We note that the ratio $(W_0^{cl})_{pred}/(W_0^{cl})$ gives the coefficient of decrease of the partial half-life $T_{1/2}^{\alpha}$.

The isotopes ^{218}Ac, ^{207}At, and ^{205}Po have anomalously large experimental cluster spectroscopic factors, the values of which, $-\log W_0^{cl} = 2.09$, 3.30, and 3.15, lead to hindrance factors $HF_0^Z = 0.3$, $HF_0^N = 0.4$, $HF_0^Z = 0.7$, and $HF_0^N = 0.7$, respectively, these differing significantly from the systematics of the experimental and theoretical values of $HF_0^{Z,N}$.

At the same time, the isotopes ^{215}Ac and ^{187}Pb have anomalously low values of W_0^{cl} ($-\log W_0^{cl} = 2.92$ and 3.63), to which there correspond hindrance factors $HF_0^Z = 2.3$ and $HF_0^N = 10$, which deviate strongly from the systematics for all the considered cases. Note that the expected value, $\log W_0^{cl}(^{187}Pb) = -3.0$, leads to an estimate $\alpha(^{187}Pb) = 17\%$ of the fraction under the condition that the α transition with $E_\alpha = 6.08$ MeV is favored. Obviously, more accurate experimental data are required for the decay of ^{189}Pb, to which there corresponds the value $\log W_0^{cl} = -3.56$ (Table IV), this leading to a hindrance factor $HF_0^Z(^{190}Bi) = 0.3$, much smaller than unity. For the decay of ^{210}At, we have two favored α transitions (Table IV), and when the sum of their W_0^{cl} values is taken the effective value $HF_0^Z(^{210}At) = 2.4$ is anomalously large. For the favored α decay of ^{210}At the expected value is $\log W_0^{cl} = -3.9$.

In the case of the other odd–odd isotope ^{198}At the anomalously small value of W_0^{cl} ($\log W_0^{cl} = -3.22$) leads to significantly too large hindrance factors HF_0^Z and HF_0^N. The expected value $\log W_0^{cl} = -2.9$ can serve as an indication of the possible existence of a second favored α transition of ^{198}At, like the cases of ^{210}At and ^{212}Fr (see Sec. 3.3).

The isotope ^{192}Bi has $\log W_0^{cl} = -2.70$ and, accordingly the neutron hindrance factor $HF_0^N = 0.7$ (Table III), which does not agree with the general systematics of the hindrance factors HF_0^N. The expected value $\log W_0^{cl} = -2.9$ is close to the previous experimental value $\log W_0^{cl} = -2.86$.[51] Using the value $\log W_0^{cl}(^{192}Bi) = -2.9$ and the experimental value $\log W_0^{cl}(^{191}Pb) = -3.13$ (Table IV), we can calculate the proton hindrance factor $HF_0^Z(^{192}Bi) = 0.6$, which does not agree with the systematics. Therefore, for the isotope ^{191}Pb the value $\log W_0^{cl} = -2.85$ is preferable, and this leads to the estimate $2\times10^{-2}\%$ for the expected α-decay fraction, in agreement with the upper experimental estimate of the fraction with allowance for the error (Table IV).

In the region of the rare-earth elements, we consider ^{160}Hf, for which the value $\log W_0^{cl} = -1.99$ appears too large when compared with the $W_0^{cl}(Z, N)$ systematics. There are also anomalous characteristics for the favored α decay of ^{148}Sm, whose experimental value $\log W_0^{cl} = -2.78$ contradicts the general tendency for $W_0^{cl}(N)$ to increase on the transition from $N = 84$ to $N = 86$.

Besides the ones considered above, there are ten further isotopes with anomalous experimental values of the cluster spectroscopic factors and hindrance factors (Tables III–V), for which correction and verification of the experimental data would be of considerable interest.

TABLE IV. Favored α transitions.

Z	N	E_α	$T_{1/2}$	α	1 for 100 α decays	$-\log W_0^{cl}$	HF_0^Z	HF_0^N	References
90	122	7802(10)	$30^{(20)}_{(10)}$ msec	~ 100 [a]	—	2.84	—	—	[63]
	123	7692(10)	150(25) msec	~ 100 [a]	—	3.20	—	2.3	[5]
	124	7682(10)	125(25) msec	~ 100	—	3.11 *	—	—	[5]
		7677(10)	80(10) msec	~ 100	—	2.92	—	—	[5]
	125	7395(8)	1.2(2) sec	100	52(3)	3.44(8)		2.2(6)	[5]
	126	7921(8)	28(2) msec	100	—	3.25(3)	—	—	[5]
	128	9680(20)	122(8) nsec	100	—	2.47(3)	—	—	[5]
		9665(10)	96(7) nsec	100(2)	—	2.36(3) *	—	—	[5]
	129	9340(20)	1.05(3) μsec	~ 100 [a]	—	2.69	—	2.1	[5]
	130	8790(20)	9.7(6) μsec	~ 100 [a]	—	2.31	—	—	[5]
89	120	7587(15)	0.10(5) sec	~ 100 [a]	—	2.99	1.2	—	[5]
	121	7462(8)	0.35(5) sec	~ 100 [a]	—	3.14	1.2	1.4	[5]
	122	7480(8)	0.25(5) sec	~ 100 [a]	—	3.09	1.1	—	[5]
	123	7379(8)	0.93(5) sec	~ 100 [a]	—	3.33	1.1	1.7	[5]
	124	7362(8)	0.80(5) sec	~ 100 [a]	—	3.22	1.4	—	[5]
	125	7214(5)	8.2(2) sec	$\geqslant$ 86	52(2)	4.09	2.8	7.3	[5]
	125	7082(5)	8.2(2) sec	$\geqslant$ 86	44(2)	3.68	1.1	2.9	[5]
	126	7604(5)	0.17(1) sec	99.91(2)	—	3.40(3)	1.07(6)	—	[5]
	128	9650(10)	111(7) nsec	~ 100 [a]	—	2.61	1.3	—	[5]
	129	9204(15)	0.27(4) μsec	~ 100 [a]	—	2.09	0.3	0.3	[5]
	130	8664(10)	7(2) μsec	~ 100 [a]	—	2.16	1.2	—	[5]
88	118	7272(5)	0.4(2) sec	~ 100 [a]	—	2.91	—	—	[5]
	119	7131(5)	1.3(2) sec	~ 100 [a]	—	2.94	—	1.1	[5]
	120	7133(5)	1.2(2) sec	~ 100 [a]	—	2.92	—	—	[5]
	121	7010(5)	4.7(2) sec	~ 100 [a]	—	3.08	—	1.5	[5]
	122	7020(5)	3.8(2) sec	~ 100 [a]	—	3.06	—	—	[5]
	123	6912(5)	15(2) sec	~ 100 [a]	—	3.27	—	1.6	[5]
	124	6902(5)	13.0(2) sec	~ 100 [a]	—	3.21	—	—	[5]
	125	6624(5)	2.75(15) min	80(5)	47(3)	3.63(3)	—	2.7(2)	[5]
	126	7138(5)	2.46(3) sec	99.941(4)	—	3.37(2)	—	—	[5]
	128	9349(8)	0.182(10) μsec	100(1)	—	2.54(2)	—	—	[5]
	129	8994(10)	1.6(2) μsec	~ 100 [a]	—	2.66	—	1.3	[5]
	130	8384(10)	14(2) μsec	~ 100 [a]	—	2.09	—	—	[5]
87	114	7388(15)	48(15) msec	~ 100 [a]	—	2.69	0.9	—	[65]
	115	7251(10)	0.34(4) sec	~ 100 [a]	—	3.09	1.3	2.6	[65]
	116	7135(10)	0.55(2) sec	~ 100 [a]	—	2.90	1.3	—	[65]
	117	7027(5)	2.1(2) sec	~ 100 [a]	70(15)	3.29	1.3	2.4	[5]
		6967(5)	2.1(2) sec	~ 100 [a]	30(6)	3.46	1.9	3.6	[5]
	118	6917(5)	3.96(4) sec	~ 100 [a]	—	3.02	1.3	—	[66]
	119	6785(5)	16.0(1) sec	85(2)	—	3.26(1)	1.3(3)	1.7	[5]
	120	6761(5)	14.8(1) sec	93(3)	—	3.12(1)	1.3(1)	—	[5]
	121	6636(5)	58.0(3) sec	74(3)	—	3.31(2)	1.6(2)	1.5(1)	[5]
	122	6646(5)	50.0(3) sec	89(3)	—	3.22(1)	1.3(2)	—	[5]
	123	6542(5)	3.18(6) min	81 [6]	—	3.49	1.3(2)	1.9	[5]
	124	6534(5)	3.10(7) min	90 [6]	—	3.38	1.1	—	[5]
	125	6383(3)	20.6(3) min	44(5)	24.0(12)	4.53(5)	6.2(8)	14	[67]
	125	6262(4)	20.6(3) min	44(5)	37(5)	3.83(7)	1.2(2)	2.8	[67]
	126	6775(5)	34.7(3) sec	99.43(3)	—	3.568(6)	1.10(5)	—	[5]
	128	9355(10)	0.12(2) μsec	~ 100	—	2.69	1.2	—	[5]
	129	9006(12)	0.70(2) μsec	~ 100 [a]	—	2.63	0.9	0.9	[5]
	130	8315(8)	22(5) μsec	~ 100 [a]	—	2.4	1.2	—	[5]
86	113	6995(10)	620(25) msec	~ 100 [a]	—	2.72	—	—	[68]
	114	6900(10)	1.06(7) sec	~ 100 [a]	—	2.72	—	—	[68]
	115	6721(8)	7.0(4) sec	~ 80 [в]	—	2.98	—	1.9(4)	[5]
	116	6636(3)	9.9(2) sec	~ 93 [в]	—	2.78	—	—	[5]
	117	6497(5)	42(2) sec	45(8)	—	3.18(8)	—	2.6(5)	[69]
	118	6417(3)	74(2) sec	72(8)	—	2.91(5)	—	—	[5]
	119	6263(3)	170(4) sec	23(5)	—	3.13(9)	—	16(4)	[5]
	120	6260(3)	5.67(17) min	64(3)	99.99	3.02(3)	—	—	[5]
	121	6126(3)	556(15) sec	23(2)	99.2	3.11(4)	—	1.2(1)	[5]
	122	6139(3)	23.5(5) min	67(3)	99.99	3.10(2)	—	—	[5]
	122	6139(3)	1464(8) sec	62(5)	99.99	3.23(4)	—	—	[5]
	123	6039(3)	28.5(10) min	17(2)	99.6	3.37(5)	—	1.8(3)	[5]
	124	6038(3)	144(6) min	96(1)	99.99	3.35(2)	—	—	[5]
	125	5783(3)	900(30) min	26(1)	63(1)	3.73(1)	—	2.4(1)	[5]
	126	6264(3)	23(1) min	100	99.95	3.53(2)	—	—	[5]
	128	9035(10)	0.27(2) μsec	100	—	2.63(3)	—	—	[5]
	129	8674(8)	2.30(10) μsec	100	—	2.67(2)	—	1.1(2)	[5]
	130	8049(10)	45(5) μsec	100	—	2.34(5)	—	—	[5]
85	111	7055(7)	0.3(1) sec	~ 100 [a]	—	3.06	1	—	[5]
	112	6959(5)	0.4(1) sec	~ 100 [a]	—	2.84	1.1	—	[5]
	113	6748(5)	4.9(5) sec	$100^{(0)}_{(10)}$	—	3.22(6)	2.1(4)	2.4	[5, 65]
	114	6639(5)	7.2(5) sec	~ 100	—	2.98	1.1	—	[5]
	115	6463(5)	42(2) sec	53(8)	60(11)	3.58(7)	2.5(4)	3.9(7)	[5]
	115	6412(5)	42(2) sec	53(8)	40(8)	3.54(6)	2.3(4)	3.6(7)	[5]
	116	6342(5)	1.50(7) min	71(7)	—	3.06(5)	1.1(2)	—	[5]
	117	6133(3)	3.0(1) min	12.0(8)	64(2)	3.50(3)	1.2(1)	2.8(4)	[69]
		6226(3)	3.0(1) min	12.0(8)	36(2)	4.26(4)	5.3(6)	12(2)	[69]
	118	6088(1)	7.4(3) min	13.8(6)	—	3.44(3)	1.7(2)	—	[5]
	119	5952(2)	9.3(3) min	4.5(4)	—	3.41(4)	1.3(3)	0.9(1)	[5]
	120	5899(4)	26.2(5) min	10(2)	—	3.28(9)	0.9(2)	—	[5]
	124	5703(2)	29.3(4) min	0.88(8)	—	3.57(4)	2.7(6)	2.0(5)	[5]
	122	5759(3)	106(3) min	10 [в]	—	3.31	0.74(6)	—	[5]
	123	5641(3)	1.63(3) h	0.55(5)	96.9(3)	4.00(11)	1.6(4)	5.0(5)	[5]
	124	5647(2)	5.41(50) h	4.1(5)	99.9	3.67(7)	1.1(2)	—	[5]
	125	5443(1)	8.3 h	0.18(2)	28.4(15)	4.75(5)	9(1)	13(4)	[67]
	125	5361(1)	8.3 h	0.18(2)	27.8(20)	4.33(6)	3.2(4)	5(1)	[67]
	126	5866(2)	7.214(7) h	41.94(50)	99.99	3.87(1)	1.10(3)	—	[5]

Continuation of Table IV.

Z	N	E_α	$T_{1/2}$	α	1 for 100 α decays	$-\log W_0^{cl}$	HF_0^Z	HF_0^N	References
	128	9080(12)	0.11(2) μsec	100	—	2.64(8)	0.8(2)	—	[5]
	130	8026(4)	0.10(2) msec	~ 100 [a]	99.95(2)	2.93	2.3	—	[5]
84	108	7170(20)	34(3) msec	$\leqslant 100$	—	2.90	—	—	[70]
	109	6940(20)	360(50) msec	~ 100 [a]	—	3.11	—	1.6	[70]
	110	6847(10)	410(30) msec	~ 100 [a]	—	2.86	—	—	[5, 70]
	111	6624(8)	4.5(5) sec	~ 100 [a]	—	3.06	—	1.6(4)	[5]
	112	6521(4)	5.5(5) sec	~ 100 [a]	—	2.79	—	—	[5]
	113	6280(5)	52(4) sec	90(10)	—	2.90(5)	—	1.3(2)	[5]
	114	6185(5)	1.78(5) min	70(8)	—	2.93(5)	—	—	[5]
	115	5952(2)	324(20) sec	12(2)	—	3.18(8)	—	1.8(4)	[5]
	116	5861(5)	675(15) sec	14(2)	—	3.02(6)	—	—	[5]
	117	5685(4)	905(25) sec	1.6(3)	—	3.27(8)	—	1.8(4)	[5]
	117	5685(4)	15.8(3) min	1.15(10)	—	3.43(4) *	—	2.6(4)	[5]
	118	5588(2)	45.0(15) min	2.00(15)	—	3.21(5)	—	—	[5]
	119	5384(3)	33(1) min	0.11(2)	—	3.31(8)	—	1.3(3)	[5]
	120	5377(1)	3.53(3) h	0.62(6)	—	3.34(4)	—	—	[5]
	121	5220(10)	1.80(4) h	0.074(16)	—	3.15(5) *	—	0.7(1)	[5]
	121	5220(10)	1.80(4) h	0.49(6)	—	2.33(5)	—	0.10(1)	[5]
	122	5224(2)	8.83 days	5.2(4)	—	3.43(3)	—	—	[5]
	123	5115(2)	5.7(3) h	0.014(3)	—	3.81(1) *	—	2.4(6)	
	123	5115(2)	5.7(3) h	0.008(1)	—	4.05(6)	—	4.2(7)	[5]
	124	5116(2)	2.8976(16) yr	99.82(1)	—	3.62(1)	—	—	[5]
	125	4882(3)	102(5) yr	99.74(3)	99.26	3.82(2)	—	1.6(1)	[5]
	126	5304.51(7)	138.3763(17) days	100	99.99	3.83(1)	—	—	[5]
	128	8784.37(7)	0.296(2) μsec	100	—	2.72(1)	—	—	[5]
	129	8375(4)	4.2(8) μsec	100	99.99	2.83(8)	—	1.3(2)	[5]
	130	7687.09(6)	164.3(17) μsec	100	—	2.56(1)	—	—	[5]
82	102	6632(10)	0.55(6) sec	~ 100	—	2.87	—	—	[53]
	103	6406(15)	4.1(3) sec	~ 100 [a]	51(5)	3.19	—	2.1	[71]
	104	6335(10)	4.7(1) sec	100	—	2.69	—	—	[53]
	105	6080(20)	17(4) sec	~ 4	—	3.63(10)	—	8.7	[5]
	106	5980(5)	22(2) sec	22(7)	—	2.59(15) *	—	—	[53]
	106	5980(10)	24.5(15) sec	3.3(11)	—	3.46(15)	—	—	[5]
	107	5720(10)	51(3) sec	0.42(15)	—	3.56(16)	—	9(5)	[5]
	108	5577(5)	1.2(1) min	0.9(2)	—	2.68(10) *	—	—	[53]
	108	5580(10)	1.2(2) min	0.21(7)	—	3.34(16)	—	—	[5]
	109	5290(20)	1.3(3) min	$1.3(5)\cdot10^{-2}$	—	3.13(20)	—	3(1)	[5]
	110	5112(5)	3.5(1) min	$5.7(10)\cdot10^{-3}$	—	2.97(8) *	—	—	[53]
	110	5112(5)	2.3(5) min	$6.9(24)\cdot10^{-3}$	—	2.67(18)	—	—	[5]
	128	3720(20)	22.26(22) yr	$1.7(3)\cdot10^{-6}$	—	3.471(8)	—	—	[5]
80	95	6860(20)	$20^{(40)}_{(13)}$ msec	~ 100 [a]	—	2.91	—	—	[72]
	96	6750(20)	$34^{(18)}_{(9)}$ msec	~ 100 [a]	—	2.78	—	—	[72]
	97	6580(10)	0.17(5) sec	~ 100 [a]	—	2.93	—	1.4	[73]
	101	6003(15)	3.6(3) sec	26(4)	87(13)	2.69(9)	—	—	[5]
	102	5867(5)	11.3(5) sec	15.2(8)	—	2.80(3)	—	—	[71]
	103	5905(15)	8.8(5) sec	10.6(2)	—	3.03(3)	—	1.7	[5]
	104	5535(15)	32.5(10) sec	1.11(6)	—	2.91(2)	—	—	[5]
	105	5652(15)	48.0(15) sec	$\geqslant 4.6$	96	3.04	—	1.3	[5]
	106	5094(15)	1.42(10) min	$1.6(5)\cdot10^{-2}$	—	2.97(14)	—	—	[5]
79	94	6720(20)	$59^{(48)}_{(18)}$ msec	~ 100 [a]	—	3.28	5.6	—	[72]
	95	6530(20)	120(2) msec	~ 100 [a]	—	2.94	2.2	0.5	[72]
	96	6440(10)	200(22) msec	~ 100 [a]	—	2.85	3.5	—	[72]
	102	5623(5)	11.5(10) sec	1.1(3)	55	3.56(12)	8.6	—	[5]
	104	5343(5)	42(4) sec	0.30(5)	—	3.17(8)	3.4	—	[5]
	105	5172(15)	53.0(14) sec	$1.1(3)\cdot10^{-2}$	—	3.77(12)	1.3	4(1)	[5]
	106	5070(15)	4.2(3) min	9.3(20)	—	3.04(3)	1.8	—	[5]
78	91	6678(15)	$2.5^{(2.5)}_{(1.0)}$ msec	~ 100 [a]	—	2.11	—	—	[74]
	92	6545(8)	$6^{(5)}_{(2)}$ msec	~ 100 [a]	—	2.05	—	—	[74]
	93	6453(4)	40(10) msec	~ 100 [a]	—	2.56	—	3.3	[75]
	94	6314(4)	120(10) msec	~ 100	—	2.54	—	—	[75]
	95	6205(3)	325(20) msec	$95^{(5)}_{(25)}$	—	2.60	—	1.1	[73,75]
	96	6043(5)	0.7(2) sec	88(10)	—	2.30(13)	—	—	[73,75]
	97	5960(10)	2.52(8) sec	55(5)	—	2.79(4)	—	3.1	[5, 73]
	98	5750(15)	6.33(15) sec	42(4)	98.6	2.42(4)	—	—	[5]
	99	5525(20)	11(2) sec	5.9(5)	—	2.51(9)	—	1.2(3)	[5]
	100	5458(5)	19(2) sec	7.5(3)	—	2.40(5)	—	—	[71]
	101	5150(10)	33(4) sec	0.27(4)	—	2.64(8)	—	1.7(4)	[5, 71]
	102	5139(19)	50(5) sec	~ 0.3	—	2.63	—	—	[5]
	103	5020(20)	51(5) sec	$\sim 6\cdot10^{-2}$	—	2.71	—	1.2	[5]
	104	4840(20)	2.6(1) min	$\sim 2.3\cdot10^{-2}$	—	2.64	—	—	[5]
	105	4730(20)	6.5(10) min	$\sim 1.3\cdot10^{-3}$	—	3.66	—	10	[5]
	106	4500(20)	17.3(2) min	$\sim 10^{-3}$	—	2.79	—	—	[5]
	108	4230(20)	2.0(1) h	$\sim 1.4\cdot10^{-4}$	—	2.72	—	—	[5]
	110	3930(10)	10.2(3) days	$3.0(6)\cdot10^{-5}$	—	3.27(8)	—	—	[5]
	112	3180(20)	$5.4(6)\cdot10^{11}$ yr	100	—	3.10	—	—	[5]
76	88	6320(20)	41(20) msec	100(70)	—	$2.83^{(57)}_{(24)}$	—	—	[74]
	89	6164(10)	$65^{(70)}_{(30)}$ msec	100(40)	—	$2.46^{(20)}_{(37)}$	—	0.4(4)	[74]
	90	5981(6)	181(38) msec	72(13)	—	2.36(12)	—	—	[74]
	91	5836(5)	1.05(35) sec	58(12)	—	2.64(17)	—	1.9(9)	[74]
	96	5105(10)	19(2) sec	$\leqslant 0.3$	—	2.91	—	—	[5]
	97	4940(10)	16.0(5) sec	$0.021^{(13)}_{(5)}$	—	3.14	—	1.7	[5]
	98	4760(10)	45(5) sec	$0.020^{(10)}_{(4)}$	—	$2.62^{(18)}_{(10)}$	—	—	[5]
	110	2760	$2.0(11)\cdot10^{-15}$ yr	100	—	$3.05^{(19)}_{(35)}$	—	—	[5]
75	88	5918(6)	260(40) msec	64(18)	—	$2.71^{(19)}_{(17)}$	1.8	—	[74]
	90	5506(10)	2.4(6) sec	13(3)	—	$2.67^{(13)}_{(18)}$	1.3	—	[74]
74	85	6299(6)	7.3(27) msec	~ 100	—	2.78	—	2.3	[74]
	86	5920(10)	81(15) msec	94(40)	—	2.45(19)	—	—	[74]

Continuation of Table IV.

Z	N	E_α	$T_{1/2}$	α	1 for 100 α decays	$-\log W_0^{cl}$	HF_0^Z	HF_0^N	References
	87	5777(5)	410(40) msec	82(26)	—	2.66(14)	—	1.6(9)	[74]
	88	5538(5)	1390(40) msec	46(4)	—	2.45(4)	—	—	[74]
	89	5384(5)	3.0(2) sec	41(5)	—	2.16(6)	—	0.5(1)	[76]
	90	5148(5)	6.4(8) sec	2.6(17)	—	$2.56^{(22)}_{(46)}$	—	—	[76]
73	84	6219(10)	5.3(18) msec	100(23)	—	2.76(18)	1,5(7)	—	[76]
	85	6051(6)	36.8(16) msec	93(6)	—	3.03(3)	2,0(3)	1.9(8)	[76]
	86	6601(6)	570(180) msec	80(5)	—	2.52(14)	1,0(4)	—	[76]
72	84	5878(10)	25(4) msec	100(19)	—	2.59(10)	—	—	[76]
	85	5735(5)	110(6) msec	91(7)	—	2.73(3)	—	1.4(4)	[76]
	86	5268(5)	3.2(6) sec	46(3)	—	2,51(9)	—	—	[76]
	87	5095(5)	5.6(5) sec	12(1)	—	2.53(5)	—	1.1(2)	[76]
	88	4777(5)	12 sec	2.3(6)	—	1,98	—	—	[76]
	102	2500(30)	$2.0(4)\cdot10^{-15}$ yr	~ 100	—	2.46	—	—	[5]
71	84	5656(6)	70(6) msec	79(4)	—	2.71(4)	1.6(2)	—	[76]
	85	5568(5)	180(20) msec	100(25)	—	2.68(12)	1.2(4)	0.92(35)	[76]
	85	5450(10)	0.5 sec	~ 70	—	2.78	1.9	1.2	[5, 76]
	86	4996(5)	4.5(15) sec	6(2)	—	2.77(21)	4(2)	—	[76]
70	84	5332(5)	410(30) msec	93(2)	—	2.50(3)	—	—	[76]
	85	5206(5)	1.59(22) sec	84(10)	—	2.60(8)	—	1.3(3)	[76]
	86	4686(10)	23(1) sec	9(2)	—	2.18(10)*	—	—	[77]
	86	4686(10)	24(1) sec	21(6)	—	1.83(13)	—	—	[76]
69	84	5109(5)	1.58(15) sec	$95^{(5)}_{(8)}$	—	2.58(5)	1.5(2)	—	[76]
	85	4959(5)	5(1) sec	44(15)	—	2.74(17)	1.4(8)	1.4(6)	[76]
	87	4234(10)	86(4) sec	$6.4(10)\cdot10^{-2}$	—	2.84(7)	0,6(2)	—	[8]
	87	4230(10)	80(3) sec	$9(3)\cdot10^{-2}$	—	2.66(15)	0.4(2)	—	[77]
68	84	4802(5)	9.8(3) sec	93(4)	—	2.38(2)	—	—	[76]
	85	4675(10)	35.6(2) sec	50(10)	—	2.58(9)	—	1.6(3)	[5, 8]
	86	4166(5)	3.75(12) min	0.47(13)	—	2.57(12)	—	—	[5]
	87	4012(5)	5.3(3) min	$2.0(7)\cdot10^{-2}$	—	3.05(15)	—	3(1)	[5]
67	84	4517(5)	36(2) sec	20(5)	—	2.68(11)	1.6(4)	—	[5]
	85	4387(5)	141.6(96) sec	12(3)	—	2.74(11)	1.5(4)	1.2(4)	[78]
	86	4010(5)	9.3(5) min	0.15(5)	—	3.03(14)	4.5(15)	—	[5]
	87	3933(5)	11.8(5) min	$1.7(4)\cdot10^{-2}$	—	3.58(10)	10(3)	3.6(15)	[5]
66	84	4232(5)	7.17(2) min	31(3)	—	2.48(6)	—	—	[5]
	85	4067(5)	16.9(5) min	5.5(8)	—	2.57(6)	—	1.2(2)	[5]
	86	3630(5)	2.37(2) h	$9.4(9)\cdot10^{-2}$	—	2.37(5)*	—	—	[5]
	86	3630(5)	2.37(2) h	$5.5(10)\cdot10^{-2}$	—	2.60(8)	—	—	[5]
	87	3464(5)	6.29(10) h	$8.3(13)\cdot10^{-3}$	—	2.57(6)	—	1.6(3)	[5]
	88	2872(5)	$1.0(4)\cdot10^{7}$ yr	100	—	3.20(20)	—	—	[5]
	88	2872(5)	$7.3(44)\cdot10^{6}$ yr	100	—	3.06(26)*	—	—	[5]
65	84	3967(3)	4.10(5) h	16.7(14)	99.99	3.24(4)	5.1(15)	—	[5]
	84	3967(3)	4.10(5) h	22.6(23)	99.99	3.11(4)	3.8(11)	—	[5]
	85	3492(5)	3.15(20) h	$3.9(30)\cdot10^{-4}$	—	$4.43^{(25)}_{(64)}$	52	16	[5]
	86	3409(5)	17.5(7) h	$9.5(15)\cdot10^{-3}$	—	3.15(7)	8(1)		[5]
64	84	3183(2)	97.5(65) yr	100	—	2.53(3)	—	—	[5]
	85	3018(5)	9.5(3) days	$4.6(15)\cdot10^{-4}$	—	2.71(14)	—	1.5(5)	[5]
	86	2715(18)	$1.78(8)\cdot10^{6}$ yr	100	—	2.23(2)	—	—	[5]
	87	2600(30)	120(20) days	$8\cdot10^{-7}$	—	2.21	—	1	[5]
	88	2140(30)	$1.08(8)\cdot10^{14}$ yr	100	—	2.25(3)	—	—	[5]
63	84	2908(5)	24.6(1) days	$1.1(8)\cdot10^{-7}$	—	$2.47^{(24)}_{(57)}$	$2.0^{(40)}_{(6)}$	—	[5, 64]
	85	2630(30)	54(1) days	$9.4(28)\cdot10^{-7}$	—	2.88(13)	3(1)	2.6	[5]
62	84	2460(20)	$7.4(15)\cdot10^{7}$ yr	100	—	2.26(9)	—	—	[5]
	85	2233(5)	$1.06(2)\cdot10^{11}$ yr	100	—	2.35(1)	—	1.2(3)	[5]
	86	1960(20)	$7(3)\cdot10^{15}$ yr	100	—	2.78(19)	—	—	[5]
61	84	2240(40)	17.7(4) yr	$2.8\cdot10^{-7}$	—	2.07	1	—	[5]
60	84	1849(3)	$2.1(4)\cdot10^{15}$ yr	100	—	2.06(8)	—	—	[5, 26]
55	59	3239(30)	0.57(2) sec	$1.8(6)\cdot10^{-2}$	—	2.53(15)	—	—	[23, 24]
53	57	3444(10)	0.65(2) sec	17(4)	—	2.23(10)	3(1)	—	[24]
52	55	3833(15)	$3.6^{(6)}_{(4)}\cdot10^{-3}$ sec	70(30)	—	$2.16^{(21)}_{(17)}$	—	—	[24]
	56	3320(20)	2.1(1) sec	68(12)	—	1.95(8)	—	—	[24]
	57	3080(15)	4.1(2) sec	3.9(13)	—	1.82(15)	—	0.8(3)	[24]

Note. [a] The α-decay fraction is taken to be 100%; [b] calculated values of the α-decay fraction; [c] estimate; *preferred value; **the α-decay fraction has been corrected in analysis of the experimental data from Ref. 5.

CONCLUSIONS

In this paper, two main problems have been solved. First, on a unified basis and in terms of quantities that are stable with respect to the choice of the theoretical parameters, we have analyzed all the available experimental material on the α decay of heavy nuclei. This analysis has made it possible to demonstrate the internal consistency of the great bulk of the experimental data and to give predictions in the cases when an additional verification of measured quantities is expedient. Second, the α-particle cluster spectroscopic factors obtained in this analysis have been used to test the possibilities of the theory for describing the existing experimental data on α decay. The theoretical approach based on the use of the shell model with allowance for the effects of pairing and configuration mixing, and also on the previously proposed method of interpolating between the shell and cluster regions, has made it possible not only to explain and justify the classification of α transitions and the behavior of the relative probabilities of α decay and the hindrance factors but also, and more importantly, to reproduce the absolute α-decay widths.

The new definition of the hindrance factors HF proposed in the paper has made it possible to relate the classifi-

TABLE V. Predicted values of spectroscopic factors and fractions α of favored α decays.

Z	N	Experiment, $-\log W_0^{cl}$	Predictions: $-\log W_0^{cl}$	Predictions: α, %
90	129	2.69	2.54	—
89	129	2.09	2.55	—
88	129	2.66	2.51	—
85	130	2.92	2.65	—
85	128	2.64(8)	2.80	—
85	125	4.19(6)	3.90	—
85	122	3.30	3.60	5
85	118	3.44(3)	3.30	19
85	113	3.22(6)	2.90	—
84	125	3.82(2)	4.0	—
84	121	3.15(5)	3.50	0.03
82	109	3.13(20)	2.85	0.02
82	107	3.56(16)	2.90	
82	105	3.63(10)	3.00	2
74	89	2.16(6)	2.60	17
72	88	1.98	2.40	—
62	86	2.78(19)	2.2	—
				—

cation of α transitions in accordance with the HF values more closely to the mechanism of α decay and the structure of the initial and final states of the nuclei.

In the process of the detailed theoretical analysis of the experimental data we have obtained an interesting physical conclusion—the magic gap in a proton subsystem with $Z = 82$ disappears on the transition to strongly neutron-deficient nuclei for which $102 \leqslant N \leqslant 112$. This conclusion agrees with the result of Ref. 79 based on study of the behavior of the reduced α-decay widths. It is also confirmed by our examination of the dependence $Q_\alpha(N, Z)$ of the α-particle separation energy, the investigation of the details of α transitions in the Bi isotopes, and the analysis in Ref. 48 of the position of the $9/2^-$ and $1/2^+$ levels in the excitation spectra of the Bi and Tl nuclei. Attempts to explain the disappearance of the magic nature of nuclei with proton number $Z = 82$ by introducing an equilibrium deformation can be questioned in the light of the fact[62] that the lowest 2^+ states in the even–even neutron-deficient Pb isotopes lie at excitation energies around 1 MeV. This indicates a rigidity of the shape of these nuclei and forces one to consider a significant rearrangement of the self-consistent field that preserves its sphericity. Certain indications of the correctness of this last conclusion were obtained in the theoretical study of Ref. 80.

It should be emphasized that satisfactory agreement of the experimental characteristics obtained in Ref. 62 with the earlier predictions of Ref. 48 for α transitions in the neutron-deficient isotopes of bismuth confirms the fruitfulness of the method of analyzing α-decay data employed in Ref. 48.

Finally, it appears helpful to identify the most topical directions of further experimental study. First, it would be interesting to continue the study of the α decay of the neutron-deficient isotopes of thallium, lead, and bismuth with a view to making the existing information more accurate and obtaining further information on the change in nuclear properties with increasing distance from the β-stability valley. Second, with a view to a more systematic study of semi-favored and unfavored α decays, it is very important to extend the range of odd and odd–odd nuclei in which several α transitions can be detected. Third and finally, it is necessary to test experimentally the predictions made above for a number of specific nuclei.

[1]I. Perlman and J. O. Rasmussen, Al'fa-radiowktivnost' (Alpha Radioactivity; Russ. transl.), Izd. Inostr. Lit., Moscow (1964).
[2]J. Rasmussen, in: Alpha-, Beta-, and Gammy-Ray Spectroscopy (ed. K. Siegbahn), North-Holland, Amsterdam (1965) [Russ. transl. published by Atomizdat, Moscow (1969)].
[3]E. K. Hyde, I. Perlman, and G. T. Seaborg, The Nuclear Properties of the Heavy Elements, Vols. 1–3, Prentice-Hall, Englewood Cliffs, N. J. (1964) [the reference is to No. 3 of the Russian translation edited by G. N. Flerov and published by Atomizdat, Moscow (1968)].
[4]S. G. Kadmenskiĭ and V. I. Furman, Al'fa-raspad i rodstvennye yadernye reaktsii (Alpha Decay and Related Nuclear Reactions), Énergoatomizdat, Moscow (1985).
[5]Table of Isotopes, 7th Ed. (eds. C. M. Lederer, V. S. Shirley, E. Browne, *et al.*), Wiley, New York (1978).
[6]V. G. Sołov'ev, Teoriya atomnogo yadra (Theory of the Atomic Nucleus), Énergoizdat, Moscow (1981).
[7]P. Hornshoj, P. G. Hansen, B. Jonson, *et al.*, Nucl. Phys. **A230**, 365 (1974).
[8]V. P. Afanas'ev, L. Kh. Batist, É. I. Berlovich, *et al.*, Preprint No. 532 [in Russian], Leningrad Institute of Nuclear Physics (1979).
[9]H. J. Mang, Z. Phys. **148**, 572 (1957); Phys. Rev. **119**, 1069 (1960).
[10]J. Rasmussen, Phys. Rev. **113**, 1593 (1959); **115**, 1675 (1959).
[11]J. Rasmussen, Nucl. Phys. **44**, 93 (1963).
[12]H. D. Zeh, Z. Phys. **175**, 490 (1963); H. D. Zeh and H. J. Mang Nucl. Phys. **29**, 529 (1962).
[13]K. Harada, Prog. Theor. Phys. **26**, 667 (1961).
[14]N. Carjan and A. Sandulescu, Z. Naturforsch. Teil A **313**, 1389 (1971).
[15]K. Harada and E. A. Rauscher, Phys. Rev. **169**, 818 (1968).
[16]S. G. Kadmenskiĭ and V. E. Kalechits, Yad. Fiz. **12**, 70 (1970) [Sov. J. Nucl. Phys. **12**, 37 (1971)].
[17]S. G. Kadmenskiĭ, V. E. Kalechits, and A. A. Martynov, Yad. Fiz. **16**, 717 (1972); **17**, 75 (1973) [Sov. J. Nucl. Phys. **16**, 400 (1973); **17**, 39 (1973)].
[18]V. I. Furman, S. Holan, S. G. Kadmensky, *et al.*, Nucl. Phys. **A226**, 131 (1974).
[19]S. G. Kadmenskiĭ and V. I. Furman, Fiz. Elem. Chastits At. Yadra **6**, 469 (1975) [Sov. J. Part. Nucl. **6**, 189 (1975)].
[20]S. G. Kadmenskiĭ and V. I. Furman, in: Materialy XIII Zimneĭ shkoly LIYaF (Proc. of the 13th Winter School of the Leningrad Institute of Nuclear Physics), Leningrad Institute of Nuclear Physics (1978), p. 59.
[21]V. I. Furman, S. Holan, S. G. Kadmensky, and G. Stratan, Preprint E4-11286 [in English], JINR, Dubna (1978).
[22]S G. Kadmensky, Z. Phys. A **312**, 113 (1983).
[23]E. Roeckl, G. M. Gowdy, and R. Kirchner, *et al.*, Z. Phys. A **294**, 221 (1980).
[24]D. Schardt, T. Batsch, and R. Kirchner, *et al.*, Nucl. Phys. **A368**, 153 (1981).
[25]V. A. Kravtsov, Massy atomov i énergii svyazi yader (Atomic Masses and Nuclear Binding Energies), Atomizdat, Moscow (1974).
[26]A. H. Wapstra and K. Bos, At. Data Nucl. Data Tables **19**, 177 (1977).
[27]G. Gamov, Z. Phys. **51**, 204 (1928).
[28]E. V. Condon and R. W. Gurney, Nature **122**, 439 (1928).
[29]A. M. Lane and R. G. Thomas, Rev. Mod. Phys. **30**, 257 (1958) [Russ. transl. published as a book, Izd. Inostr. Lit., Moscow (1960)].
[30]R. Thomas, Prog. Theor. Phys. **12**, 253 (1954).

[31]G. Igo, Phys. Rev. **115**, 1665 (1959).
[32]V. G. Kadmenskiĭ, S. G. Kadmenskiĭ, V. G. Khlebostroev, *et al.*, Acta Phys. Pol. **B13**, 885 (1982).
[33]S. G. Kadmenskiĭ, S. D. Kurgalin, V. I. Furman, *et al.*, Yad. Fiz. **33**, 573 (1981) [Sov. J. Nucl. Phys. **33**, 298 (1981)].
[34]Yu. P. Popov, Fiz. Elem. Chastits At. Yadra **13**, 1165 (1982) [Sov. J. Part. Nucl. **13**, 483 (1982)].
[35]G. R. Satchler and W. G. Love, Phys. Rep. **55**, 183 (1979).
[36]P. O. Fröman, K. Dan. Vidensk. Selsk. Mat.-Fys. Medd. **1**, N3 (1957).
[37]V. G. Nosov, Yad. Fiz. **6**, 44 (1967) [Sov. J. Nucl. Phys. **6**, 32 (1967)].
[38]A. Bohr and B. R. Mottelson, Nuclear Structure, Vol. 2, Bejamin, Reading, Mass. (1975) [Russ. transl. published by Mir, Moscow (1977)].
[39]S. G. Kadmenskiĭ, Yu- L. Ratis, V. I. Furman, *et al.*, Yad. Fiz. **27**, 630 (1978) [Sov. J. Nucl. Phys. **27**, 337 (1978)].
[40]S. G. Kadmenskiĭ and S. D. Kurgalin, Izv. Akad. Nauk SSSR Ser. Fiz. **49**, 1966 (1980).
[41]V. G. Solov'ev, Dokl. Akad. Nauk SSSR **144**, 1281 (1962) [Sov. Phys. Dokl. 7, 548 (1962)].
[42]H. J. Mang and J. O. Rasmussen, K. Dan. Vidensk. Selsk. Mat.-Fys. Medd. **2**, N3 (1962).
[43]S. G. Kadmenskiĭ and K. S. Rybak, Yad. Fiz. **19**, 971 (1974) [Sov. J. Nucl. Phys. **19**, 499 (1974)].
[44]S. G. Kadmenskiĭ, K. S. Rybak, and V. I. Furman, Yad. Fiz. **24**, 501 (1976); **27**, 906 (1978) [Sov. J. Nucl. Phys. **24**, 260 (1976); **27**, 481 (1978)].
[45]A. B. Migdal, Teoriya konechnykh fermi-sistem i svoĭstva atomnykh yader, Nauka, Moscow (1966); English transl.: Theory of Finite Fermi Systems and Applications to Atomic Nuclei, Interscience, New York (1967).
[46]I. Tonozuka and A. Arima, Nucl. Phys. **A323**, 45 (1979).
[47]K. Ya. Gromov, N. A. Golovkov, V. M. Vakhtel', *et al.*, in: Materialy 15 soveshchaniya po yadernoĭ spektroskopii i teorii atomnogo yadra (Proc. of the 15th Symposium on Nuclear Spectroscopy and Nuclear Theory), D6-11574, JINR, Dubna (1978), p. 53.
[48]V. M. Vakhtel', S. G. Kadmenskiĭ, A. A. Martynov, *et al.*, Yad. Fiz. **28**, 1241 (1978) [Sov. J. Nucl. Phys. **28**, 639 (1978)].
[49]E. P. Grigor'ev and V. G. Solov'ev, Struktura chetnykh deformirovannykh yader (Structure of Even Deformed Nuclei), Nauka, Moscow (1974).
[50]J. O. Newton, F. S. Stephens, and R. M. Diamond, Nucl. Phys. **A236**, 225 (1974).
[51]V. De Viklavik, Sh. V'e, and I. S. Dionisio, Izv. Akad. Nauk SSSR Ser. Fiz. **40**, 2057 (1976).
[52]S. A. Artamonov, V. I. Isakov, S. G. Ogloblin, *et al.*, Yad. Fiz. **39**, 328 (1984) [Sov. J. Nucl. Phys. **39**, 206 (1984)].
[53]K. S. Toth, Y. A. Ellis-Akovali, C. R. Bingham, *et al.*, Proc. of AMCO-7, Darmstadt (1984), p. 265.
[54]V. G. Chumin, V. M. Vakhtel', S. G. Kadmenskiĭ, *et al.*, see Ref. 47, p. 47.
[55]V. M. Vakhtel', N. A. Golovkov, R. B. Ivanov, *et al.*, Izv. Akad. Nauk SSSR Ser. Fiz. **45**, 1966 (1981).
[56]V.V. M. Vakhtel', S. G. Kadmenskiĭ, I. A. Lomachenkov, *et al.*, Yad. Fiz. **38**, 1403 (1983) [Sov. J. Nucl. Phys. **38**, 853 (1983)].
[57]A. A. Shihab-Eldin, L. J. Jardine, and J. R. Rasmussen, Nucl. Phys. **A244**, 435 (1975).
[58]V. I. Furman, S. Holan, and G. Stratan, Preprint E4-11287 [in English], JINR, Dubna (1978).
[59]S. A. Artamonov, V. I. Isakov, S. G. Kadmenskiĭ, *et al.*, Yad. Fiz. **36**, 829 (1982) [Sov. J. Nucl. Phys. **36**, 486 (1982)].
[60]C. W. Ma and W. W. True, Phys. Rev. C **8**, 2313 (1973).
[61]V. I. Isakov, S. A. Artamonov, and L. A. Sliv, Izv. Akad. Nauk SSSR Ser. Fiz. **41**, 2074 (1977).
[62]E. Coenen, K. Deneffe, M. Huyse, *et al.*, in: Proc. of the Seventh Intern. Conf. on Atomic Masses, AMCO-7, Darmstadt (1984), p. 272.
[63]D. Vermeulen, H. G. Clerc, W. Lang, *et al.*, Z. Phys. A **294**, 149 (1980).
[64]J. J. Hagan, Radiochim. Acta **27**, 73 (1980).
[65]G. T. Ewan, E. Hagberg, B. Jonson, *et al.*, Z. Phys. A **296**, 223 (1980).
[66]B. G. Ritchie K. S. Toth, H. K. Carter, *et al.*, Phys. Rev. C **23**, 2342 (1981).
[67]V. M. Vakhtel', N. A. Golovkov, R. B. Ivanov, *et al.*, Izv. Akad. Nauk SSSR Ser. Yiz. **45**, 1861 (1981).
[68]F. Calaprice, G. T. Ewan, and R. D. Dincklage, Phys. Rev. C **30**, 1671 (1985).
[69]H. Gauvin, Y. Le Beyec, L. Livet, *et al.*, Ann. Phys. (N.Y.) **9**, 241 (1975).
[70]M. E. Leino, S. Yashita, and A. Ghiorso, Phys. Rev. C **24**, 2370 (1981).
[71]U. J. Schrewe, P. Tidemand-Petersson, G. M. Gowdy, *et al.*, Phys. Lett. **B91**, 46 (1980).
[72]J. R. H. Schneider, S. Hofman, F. P. Hepberger, *et al.*, Z. Phys. A **312**, 21 (1983).
[73]P. Hornshoj, P. G. Hansen, E. Hagberg, *et al.*, in: Proc. of the Third Intern. Conf. on Nuclei Far from Stability, 12–26 May 1976, Geneva (1976), p. 171.
[74]S. Hofman, G. Münzenberg, F. P. Hepberger, *et al.*, Z. Phys. A **299**, 281 (1981).
[75]S. Della Negra, C. Deprun, D. Jacquet, *et al.*, Z. Phys. A **300**, 251 (1981).
[76]S. Hofman, W. Faust, G. Münzenberg, *et al.*, Z. Phys. A **291**, 53 (1979).
[77]K. S. Toth, Y. A. Ellis-Akovali, D. M. Moltz, *et al.*, Phys. Lett. **B117**, 11 (1982).
[78]E. Hagberg, P. G. Hansen, J. C. Hardy, *et al.*, Nucl. Phys. **A293**, 1 (1977).
[79]K. Toth, Y. A. Ellis-Akovali, C. R. Bingham, *et al.*, Phys. Rev. Lett. **53**, 1623 (1984).
[80]R. A. Sorensen, Nucl. Phys. **A420**, 221 (1984).

Translated by Julian B. Barbour